OPEN ACCESS
CellPress

Cell Reports
Report

# The APC Network Regulates the Removal of Mutated Cells from Colonic Crypts

Je-Hoon Song,[1] David J. Huels,[2] Rachel A. Ridgway,[2] Owen J. Sansom,[2] Boris N. Kholodenko,[3,4,5] Walter Kolch,[3,4,5] and Kwang-Hyun Cho[1,*]

[1]Department of Bio and Brain Engineering, Korea Advanced Institute of Science and Technology (KAIST), 291 Daehak-ro, Yuseong-gu, Daejeon 305-701, Republic of Korea
[2]The Beatson Institute for Cancer Research, Garscube Estate, Glasgow G61 1BD, UK
[3]Systems Biology Ireland, University College Dublin, Belfield, Dublin 4, Ireland
[4]Conway Institute of Biomolecular and Biomedical Research, University College Dublin, Belfield, Dublin 4, Ireland
[5]School of Medicine and Medical Science, University College Dublin, Belfield, Dublin 4, Ireland
*Correspondence: ckh@kaist.ac.kr
http://dx.doi.org/10.1016/j.celrep.2014.02.043


## SUMMARY

**Self-renewal is essential for multicellular organisms but carries the risk of somatic mutations that can lead to cancer, which is particularly critical for rapidly renewing tissues in a highly mutagenic environment such as the intestinal epithelium. Using computational modeling and in vivo experimentation, we have analyzed how adenomatous polyposis coli (APC) mutations and β-catenin aberrations affect the maintenance of mutant cells in colonic crypts. The increasing abundance of APC along the crypt axis forms a gradient of cellular adhesion that causes more proliferative cells to accelerate their movement toward the top of the crypt, where they are shed into the lumen. Thus, the normal crypt can efficiently eliminate β-catenin mutant cells, whereas APC mutations favor retention. Together, the molecular design of the APC/β-catenin signaling network integrates cell proliferation and migration dynamics to translate intracellular signal processing and protein gradients along the crypt into intercellular interactions and whole-crypt physiological or pathological behavior.**

## INTRODUCTION

Although self-renewal is essential for multicellular organisms, it bears the risk of mutations, in particular, in environments with high concentrations of mutagens such as the colon (Azcárate-Peril et al., 2011; Diggs et al., 2011; Pearson et al., 2009). The human colorectal epithelium is renewed every 2–3 days (Okamoto and Watanabe, 2004) making it a vulnerable target for carcinogenesis, and colorectal cancer (CRC) is the third most frequent cancer worldwide (Ferlay et al., 2010). The regeneration of the colorectal epithelium is maintained by a proliferating unit termed crypt (Humphries and Wright, 2008). The adult colon contains $10^7$ crypts, and each crypt consists of 1,000–4,000 cells. In order to regenerate such a huge cell population over many decades without malignant aberrations, crypts may have evolved mechanisms to minimize the cancer risk. Such strategies may include the spatiotemporal organization of cell proliferation, migration, and differentiation (Gatenby et al., 2010; Nowak et al., 2003). Cancer prevention being a built-in design feature of epithelial anatomy is an attractive hypothesis, but the molecular mechanisms remain to be elucidated.

Crypt cell proliferation is controlled by a spatial gradient of extracellular Wnt ligands, which causes the differential distribution of proliferative cells along the crypt axis (Davies et al., 2008; Murray et al., 2010; van de Wetering et al., 2002). In the absence of Wnt, cytoplasmic β-catenin is constantly degraded by the destruction complex (DC), which is composed of Axin, adenomatous polyposis coli (APC), and GSK3β. Binding of Wnt to its receptor Frizzled inhibits the DC, leading to the stabilization of β-catenin, which translocates to the nucleus and in conjunction with T cell factor/lymphoid enhancer factor (TCF/LEF) regulates the transcription of >100 genes that control cell proliferation. On the other hand, β-catenin can bind to E-cadherin forming an adhesion complex that controls cell-cell adhesion and migration. Such dual functions of β-catenin imply an integrated regulation of proliferation and migration for maintaining the homeostasis of crypt cells, which so far were analyzed in separation.

APC mutation in the Wnt pathway is the earliest genetic alteration in CRC (Powell et al., 1992), but it takes years to decades for a cancer to develop (Fearon, 2011). Germline APC mutations cause familial adenomatous polyposis (FAP), which eventually results in CRC in the third to fifth decade of life. This long latency suggests a robust tumor defense that may include the requirement for additional mutations, a residual tumor suppressive function of mutated APC, and the effective elimination of mutated cells (Fearon, 2011; Muzny et al., 2012; Segditsas and Tomlinson, 2006). Although the analysis of accumulating mutations has dominated the field, tumor suppressive mechanisms are equally important. For instance, Wnt activation during CRC pathogenesis occurs in two steps, the first being APC mutation, whereas the second seems to optimize the transcriptional output of Wnt signaling for tumor progression (Najdi et al., 2011). APC mutations promote β-catenin translocation to the nucleus (Sansom et al., 2004), although the quantitative extent is modulated

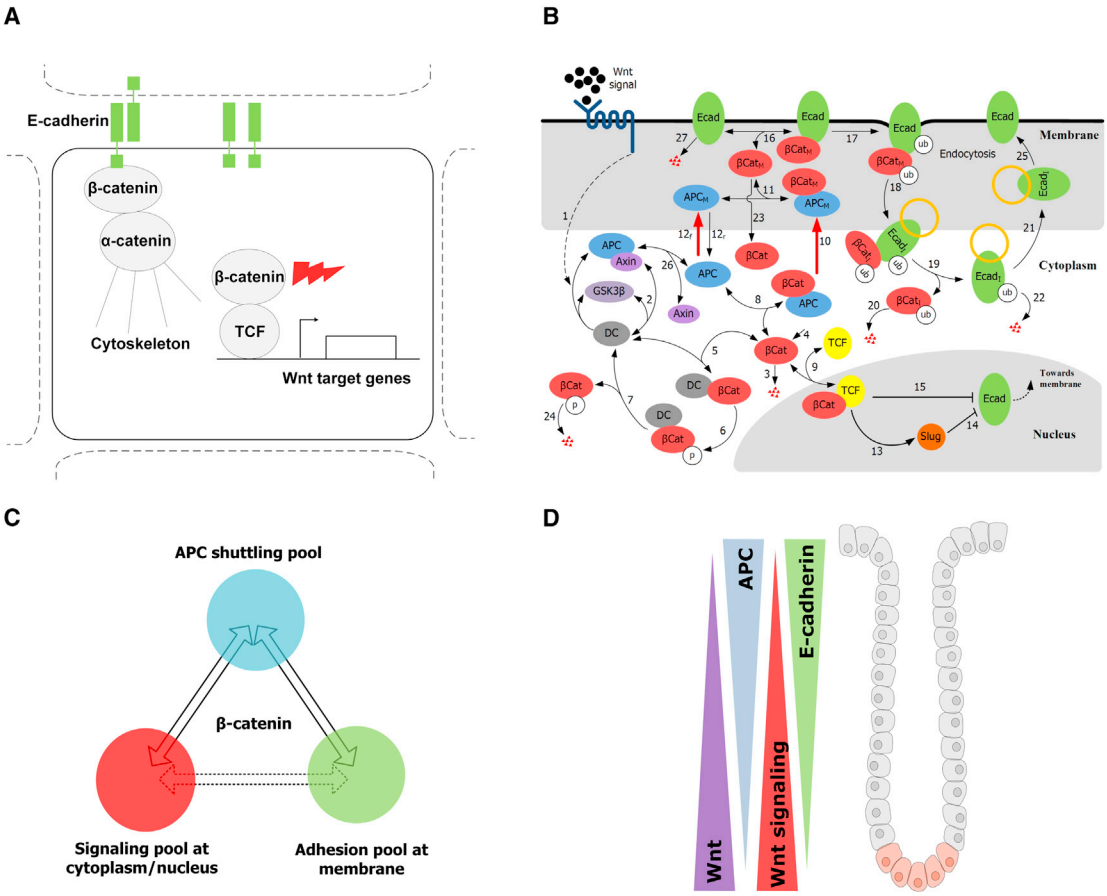


**Figure 1. Scheme of the Mathematical β-Catenin Model and Factors Considered in the Construction of the Model**

(A) Schematic diagram showing that β-catenin is a key component of both the Wnt signaling pathway and the E-cadherin cell adhesion complex.

(B) A reaction scheme of our mathematical model, which consists of β-catenin destruction, β-catenin/TCF nuclear signaling, APC shuttling, and adhesion complex remodeling.

(C) β-catenin exchanges between three distinct molecular pools within a cell.

(D) Molecular gradients within the colonic crypt. Stem cells (red) at the bottom of the crypt replenish colonic epithelial cells (gray) that differentiate as they move upward.

by other, poorly understood factors. APC mutated tumors retain membrane β-catenin comparable to normal epithelium in the tumor center, whereas cells at the invasive front show nuclear β-catenin (Brabletz et al., 1998; Phelps et al., 2009). This observation suggests that the effects of mutations are modulated by a dynamic competition between tumor promoting and suppressive forces that may depend on the signaling status of individual cells and their local microenvironment.

To analyze this hypothesis, we integrated all available experimental evidence and developed a mathematical model that allowed us to simulate the coordination between the adhesion and signaling function of β-catenin, and the adhesion and migration of single cells in normal, β-catenin, and APC mutated colonic crypts. Our results reveal a tumor suppressing function arising from the interactions between dynamic subcellular APC network and the adhesion gradient in the crypt, which promotes the elimination of mutant cells with high Wnt signaling. Subversion of these interactions permits mutant cells to persist in the crypt and initiate CRC.

## RESULTS

### Construction of a Mathematical Model for the Dynamic Analysis of Multiple β-Catenin Functions

We developed a mathematical model (Figure 1) that allowed us to investigate the dynamics of (1) the Wnt signaling pathway and resulting suppression of E-cadherin transcription; (2) the formation of functional E-cadherin-β-catenin adhesion complexes at the cell membrane; (3) the removal and recycling of E-cadherin-β-catenin adhesion complexes by endocytosis; and (4) the role of APC in coordinating the participation of β-catenin in adhesion versus Wnt signaling (see Supplemental Results for details).

We report the following key features of Wnt-E-cadherin system. First, the premise that β-catenin can be removed by degradation from the adhesion pool, but not from the signaling pool establishes a continuous flux of β-catenin from the signaling to the adhesion pool, which counterbalances the Wnt-induced formation of the β-catenin:TCF complex (Figure 2). This explains the

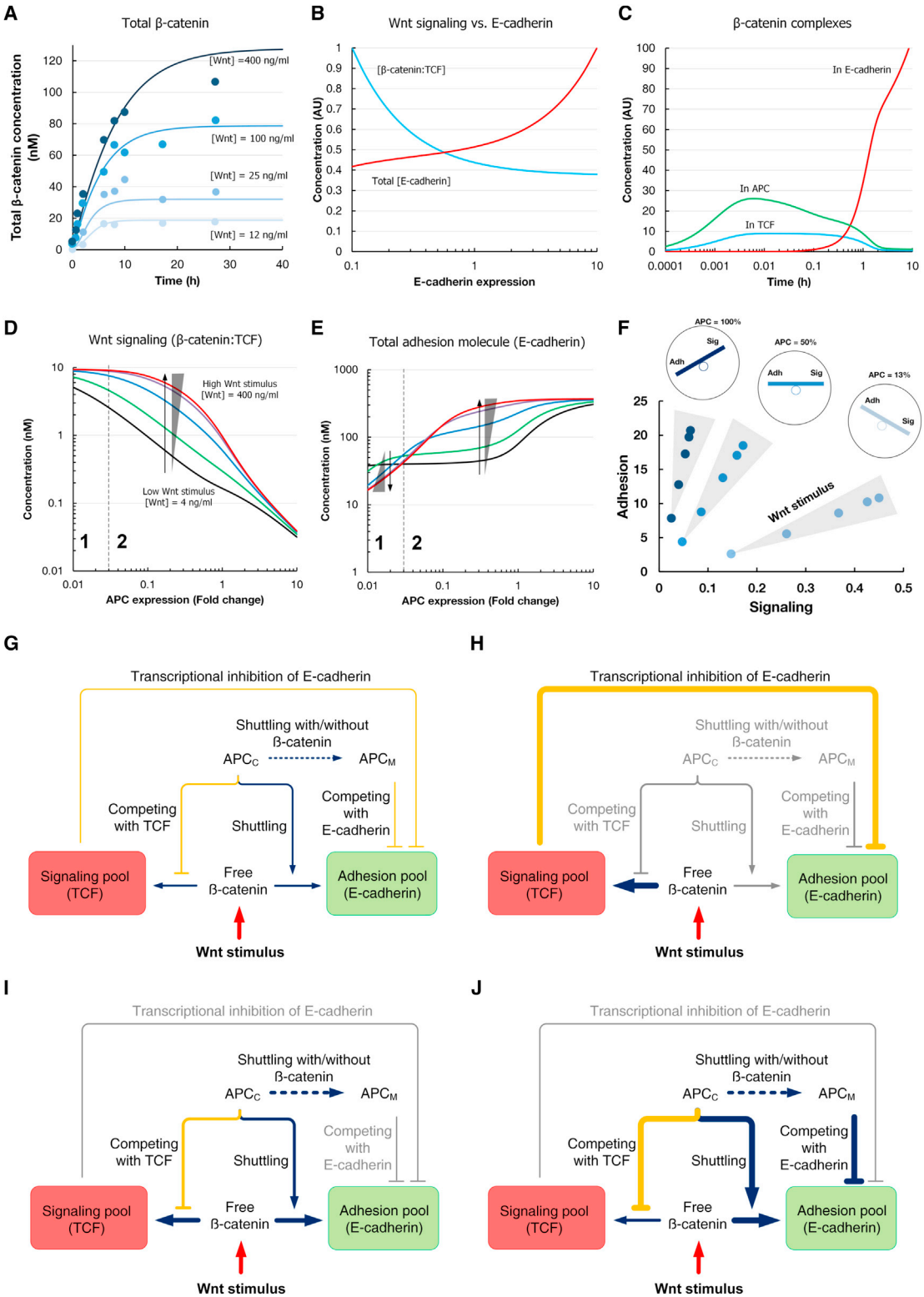


**Figure 2. APC Regulates the Distribution of β-Catenin between Signaling and Adhesion Pools**

(A) Profiles of β-catenin abundance in response to Wnt stimulation in E-cadherin-negative cells.

(B) Increasing E-cadherin expression ($A_E$) represses Wnt signaling by decreasing the abundance of the β-catenin:TCF complex.

*(legend continued on next page)*

experimental observation that E-cadherin can downregulate the signaling function of β-catenin even when a Wnt stimulus is present (Herzig et al., 2007). Second, the stimulatory effect of Wnt signaling on adhesion complex formation arises from the effect that the basal level degradation rate of E-cadherin is higher than that of ubiquitinated E-cadherin (or of complexed E-cadherin), so that its binding to β-catenin protects E-cadherin from degradation (Figure 2E). Third, the ratio of β-catenin within signaling complex to that within adhesion complex is controlled by APC expression levels (Figure 2F) (see Supplemental Results for details).

We further extended our analysis of cellular dynamics to the level of simulating cell migration within a crypt by constructing a mathematical model of "individually migrating cell" (IMC) (Figures 3A–3C). We confirmed that the IMC model could reproduce the changes in Wnt signaling (as measured by the formation of the β-catenin:TCF complex), E-cadherin, and β-catenin expression profiles along the crypt that are consistent with experimental observations (Figures 3D–3F, 3H, and 3I). We found that the increasing profile of APC plays an essential role in establishing the molecular profiles (β-catenin, E-cadherin, and Wnt activity), and that the adhesion (as measured by the formation of the β-catenin:E-cadherin complex) increased along the crypt axis, whereas the Wnt signaling decreased (first row of Figure 4B and Figures 3G and 3J) (see Supplemental Results for details).

## Spatial Signaling and Adhesion Gradients in the Crypt Facilitate the Elimination of Mutated Cells with a High Proliferative Potential

In particular, we investigated the effect of somatic mutations that enhance Wnt signaling and result in cells with a higher proliferative potential than normal neighboring cells (see Figures S4A and S4B for mutation models). Such mutations can also change the amount of adhesion complexes within a cell and subsequently induce a different adhesion level between the mutated cell and its normal neighboring cells. To investigate the effect of this "adhesion difference," we employed a force model based on the differential adhesion (see Supplemental Experimental Procedures), which posits that cells rearrange their positions to minimize the total sum of their adhesion differences (Figure 3C).

We investigated the effect of somatic mutations on a normal crypt (Figure S4B). The de novo synthesis rate of β-catenin ($k_4$) was perturbed to mimic mutations that enhance Wnt signaling. The model predicted that both signaling and adhesion increase in the mutated cell at every different height of crypt in accord with cell-level results (Figure 2F; first row of Figure 4D). The mutated cell experiences an additional force to move upward because increased adhesion causes an adhesion difference between the mutated cell and its normal neighbors (first rows of Figures 4E and 4F). As a result, mutated somatic cells with enhanced proliferation are expelled from the crypt more quickly than normal cells.

Next, we investigated the effects of APC mutations on stem cells. According to the studies about hereditary colorectal cancer syndromes, APC mutations predispose to CRC, but further alterations are required to cause full malignant transformation, and a key event in this process seems to be the acquisition of the "just right" level of Wnt signaling (Gaspar and Fodde, 2004; Minde et al., 2011; Segditsas and Tomlinson, 2006). Therefore, we simulated the effects of APC mutations in crypt stem cells on the adhesion gradient. As most APC mutations are truncations that can reduce function to different degrees (Cho et al., 2006; Fodde et al., 2001; Gaspar and Fodde, 2004), we considered three cases where the maximum APC expression and function ($APC_{Max}$) is reduced to 50%, 12%, and 3%, respectively, of its wild-type value (second to fourth rows of Figure 4). The expression profiles of β-catenin and E-cadherin progressively reversed from increasing toward the top of the crypt in wild-type APC crypts to a decrease as APC function was reduced (Figure 4A). These changes correlated with a decrease in the β-catenin adhesion pool, whereas the β-catenin signaling pool was increased (Figure 4B). Thus, a decline in APC function selectively disturbs the adhesion profile of the crypt abolishing the normal adhesion gradient when APC function is reduced by 50%, and even reversing it when APC function is 12% or less. Importantly, if a cell in the mutated crypt had experienced an additional Wnt pathway stimulation the adhesion difference, $A_1(x) - A_0(x)$ still remained positive (second to fourth rows in Figure 4D). So, the enhancement of adhesion by additional β-catenin (due to APC shuttling and the increase of the total number of adhesion molecules [Figure 2E]) is maintained even for the variation of APC function. This means that the cell still would move with the adhesion gradient and reverse direction with the gradient because the reversed adhesion gradient also reverses the direction of the force (second to fourth rows in Figures 4E and 4F). In the case of a crypt where loss of APC function had reversed the adhesion gradient, such an additional Wnt stimulation would counteract the elimination of the affected cell. Based on these results, we suggest that spatial signaling and adhesion

(C) Profile of the temporal relaxation dynamics of β-catenin distribution into its different functional protein complexes under unperturbed conditions (i.e., no Wnt signal and no APC mutations).

(D and E) Steady states of the concentrations of (D) the β-catenin:TCF complex, and (E) total E-cadherin are plotted in dependence of APC expression and Wnt stimulation. Zones 1 and 2 indicate regions that represent distinct response modes to Wnt stimulation. Black line, low Wnt stimulus; green/blue/magenta lines, increasing Wnt stimulus; red line, high Wnt stimulus; arrows in (E), increasing directions of Wnt stimulations in zones 1 and 2, respectively.

(F) Pairs of signaling and adhesion functionalities in response to Wnt stimulus are traced on the phase plane.

(G–J) The dynamic regulation of the balance between the signaling and adhesion pools. (G) The competition between E-cadherin and TCF for binding with β-catenin results in a mutually inhibitory effect between signaling and adhesion functions. The competition is balanced by the efficiency of APC shuttling. In cells with wild-type APC, β-catenin is efficiently transported to the membrane by APC where β-catenin is sequestered in a complex with E-cadherin. If the concentration of functional APC is decreased, e.g., due to mutation, TCF binding to β-catenin increases the transcription of Slug, which suppresses E-cadherin gene expression. (H) For a low level of APC expression, the increased signaling complex by extracellular Wnt stimulus transcriptionally inhibits E-cadherin. (I) For a middle level of APC expression, Wnt stimulus increases both signaling complex and adhesion complex. (J) For a high level of APC expression, APC decreases both signaling and adhesion sensitivities to Wnt stimulus.

See also Figures S1 and S2.

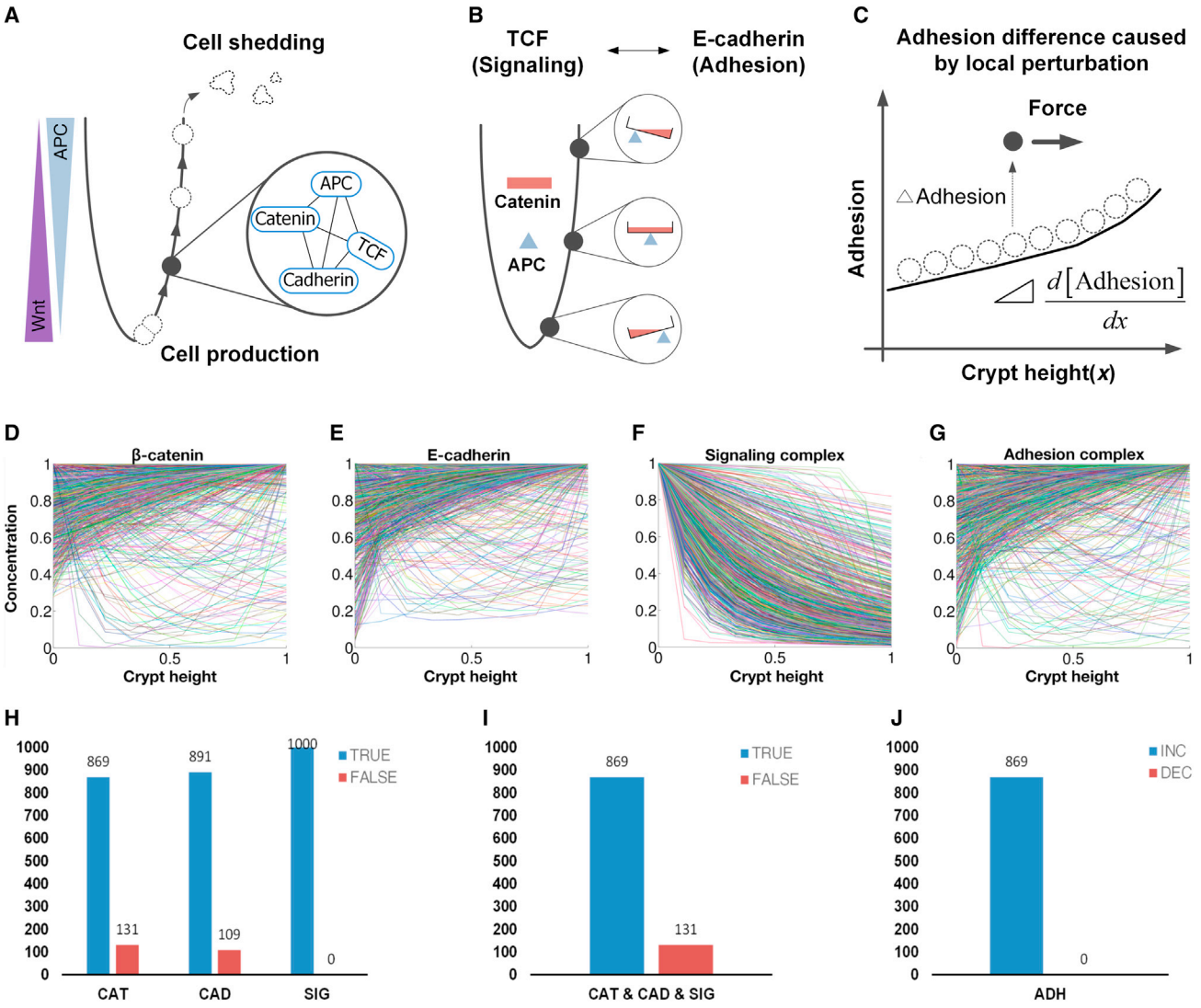


**Figure 3. Model of an Individually Migrating Cell Moving up the Crypt**

(A) The individually migrating cell (IMC) model assumes that a normal cell is autonomously migrating up the crypt. Therefore, their regulation of the intracellular β-catenin interaction network changes depending on the position of the IMC in the crypt.

(B) Schematic illustration of the balancing role of APC in a crypt. APC negatively regulates the β-catenin:TCF complex, but positively regulates the β-catenin:E-cadherin complex. Thus, the differential APC expression along the crypt controls the functional balance between signaling and adhesion.

(C) A force model governing the position of a cell in an epithelial sheet of tissue.

(D–J) The IMC model simulation using random coefficients for APC and Wnt ligand profile. (D–G) The profiles of β-catenin (D), E-cadherin (E), signaling complex (F), and adhesion complex (G) were produced from the IMC model. (H and I) A large portion of the random coefficients successfully reproduced the qualitative pattern of the profiles along the crypt. This means that the general behavior of the IMC model well explains known experimental data. CAT, CAD, SIG, and ADH indicate the profiles of β-catenin, E-cadherin, signaling complex (β-catenin:TCF), and adhesion complex (β-catenin:E-cadherin), respectively. TRUE or FALSE indicates if the reproduced profile(s) qualitatively fits experimental data or does not fit. (J) The IMC model predicts the amount of adhesion complex is increasing along the crypt.

See also Figure S3.

gradients in the crypt facilitate the elimination of mutated cells (see Supplemental Results; Figures S4C–S4E).

## Simulations of WT, APC, and β-Catenin Mutated Crypts Based on a Heterogeneous Cell Population

Our model suggests that the crypt structure enables the elimination of mutated cells that have an abnormally higher proliferation rate. To allow us to investigate this phenomenon in in vivo models, we extended this model by considering the endogenous heterogeneity of cells, which has been widely observed in various cellular contexts. In particular, we investigated the effect of heterogeneous β-catenin expression on Wnt signaling and adhesion, and the resulting repositioning of crypt cells. For this purpose, we considered a set of cells evenly sampled along

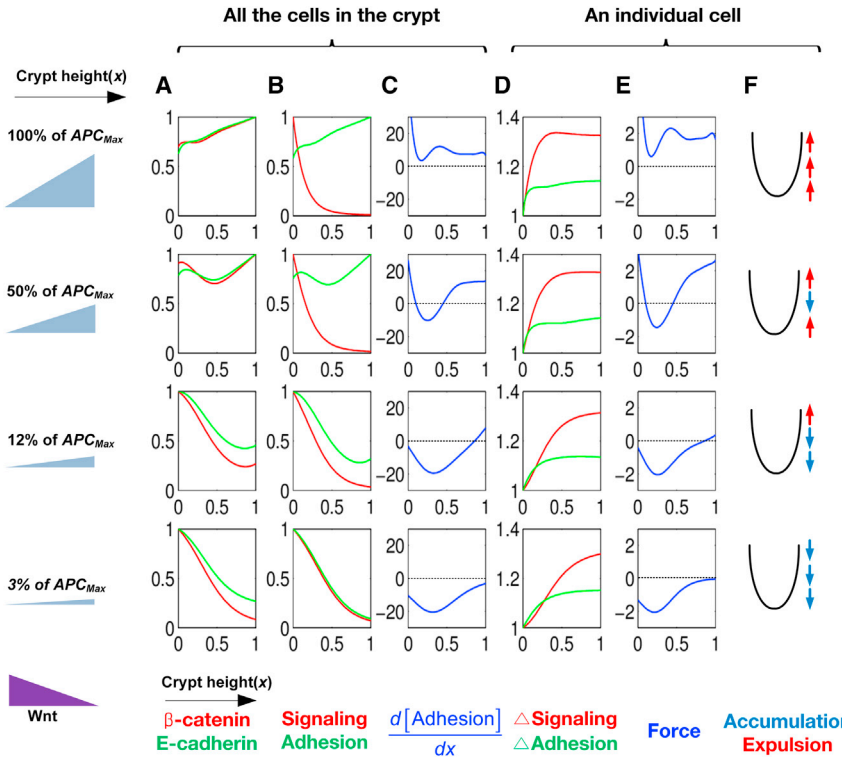


**Figure 4. Simulations of the IMC Model**

Simulations of the IMC model for wild-type (first row) and APC mutated (second to fourth rows) crypts. (A) and (B) are without additional Wnt stimulation and (D) is with additional Wnt stimulation. The additional Wnt stimulation is applied to mimic a cell with a higher proliferative potential.

(A and B) Simulation profiles of total β-catenin (red) and total E-cadherin (green) (A), and β-catenin:TCF signaling (red) and adhesion (green) complex (B) along the crypt. The simulation profiles are concordant with previous experiments (Wnt signaling, E-cadherin, and β-catenin) in a normal crypt (first row). In APC mutated crypts (second to fourth rows), the profiles of E-cadherin (green curve in A) and E-cadherin:β-catenin (green curve in B) became increasingly reversed compared to their profiles in the normal crypt. The total β-catenin profile (red curve in A) showed a decreasing pattern in the mutated crypt unlike the increasing pattern in the normal crypt, whereas the Wnt signaling profile (red curve in B) showed the same decreasing pattern in both normal and APC mutated crypts.

(C) The adhesion gradient was calculated numerically, and each row shows the adhesion gradient that corresponds to the adhesion curve (green) in (B).

(D) The effects of increased β-catenin on single mutated cell in a normal (first row) and APC mutated crypts (second through fourth rows) on differential adhesion (Δadhesion) and signaling (Δsignaling) before and after Wnt stimulation (50% of the maximal Wnt stimulus was added to the basal Wnt profile along the crypt). As a result, both signaling and adhesion were enhanced by the increased β-catenin in normal (first row) and APC mutated (second through fourth rows) crypts.

(E) β-catenin alterations induce differential adhesion resulting in forces that drive cell migration, which is estimated by multiplying the adhesion gradient (C) and the differential adhesion (green) in (D).

(F) Schematic summary of the changes in cell migration driven by the force field analysis shown in (E).

See also Figure S4.

the crypt axis and simulated their heterogeneous β-catenin expressions by adding random noise with the normal distribution of standard deviation ($\sigma = 0.2$) to the de novo synthesis rate of β-catenin ($k_4$). Such heterogeneity of β-catenin expression affects the formation of the signaling (β-catenin:TCF) and adhesion (β-catenin:E-cadherin) complexes. The change in the signaling complex affects proliferation, whereas the change of the adhesion complex results in cellular repositioning such that the difference of adhesion among neighbor cells is minimized. The repositioning eventually affects the net migration of each crypt cell. Our simulation results show such repositioning of cells (Figure 5A, fourth column) and the redistribution of cells with a high proliferative potential (Figure 5A, third column). We found that in a normal crypt, after repositioning of the cells, cells with a higher proliferative potential shift toward an upper direction, whereas cells with a lower proliferative potential shift toward a lower direction (Figure 5A, first and third columns of the first row). The average migration distance was 0.13 (cells with a higher proliferative potential) and −0.15 (cells with a lower proliferative potential), respectively (see Supplemental Results and Table S4 for details). Consequently, an intact adhesion gradient sorted crypt cells according to their proliferation rates, and cells with a higher proliferative potential incurred a penalty of reduced lifetime in crypt as shown in Figure 4. This implicates that the wild-type crypt allows cells with a lower proliferative potential to stay longer. The molecular basis of such behavior of crypt originates from the dual function of β-catenin in Wnt signaling and adhesion (Figure 1A). For instance, the increase of β-catenin increases both Wnt signaling and adhesion. Such correlated behavior is a characteristic feature of molecular interaction networks.

Next, we investigated the effects of APC and β-catenin mutation in crypt stem cells on the repositioning of crypt cells. Interestingly, the effects of APC and β-catenin mutations were not equivalent. APC mutations mainly affected the adhesion gradient (even reversed it), whereas β-catenin mutations preferentially accelerated proliferation with a lesser effect on the adhesion gradient. For a similar mutational analysis as in Figure 4, we decreased $APC_{Max}$ by 10% (compared to its wild-type value) in the APC gradient profile to mimic a crypt having an APC mutation. We found that the fluctuations in Wnt signaling was increased by 86% (compared to wild-type), whereas that in adhesion was decreased by 69% (Figure 5A, first and second column of the second row; Supplemental Results; Table S3). As we found in Figure 4, the APC mutated crypt showed an inversion of the adhesion gradient. We also found that APC mutations increased the heterogeneity in cell proliferation rates but decreased the heterogeneity in adhesion complex formation

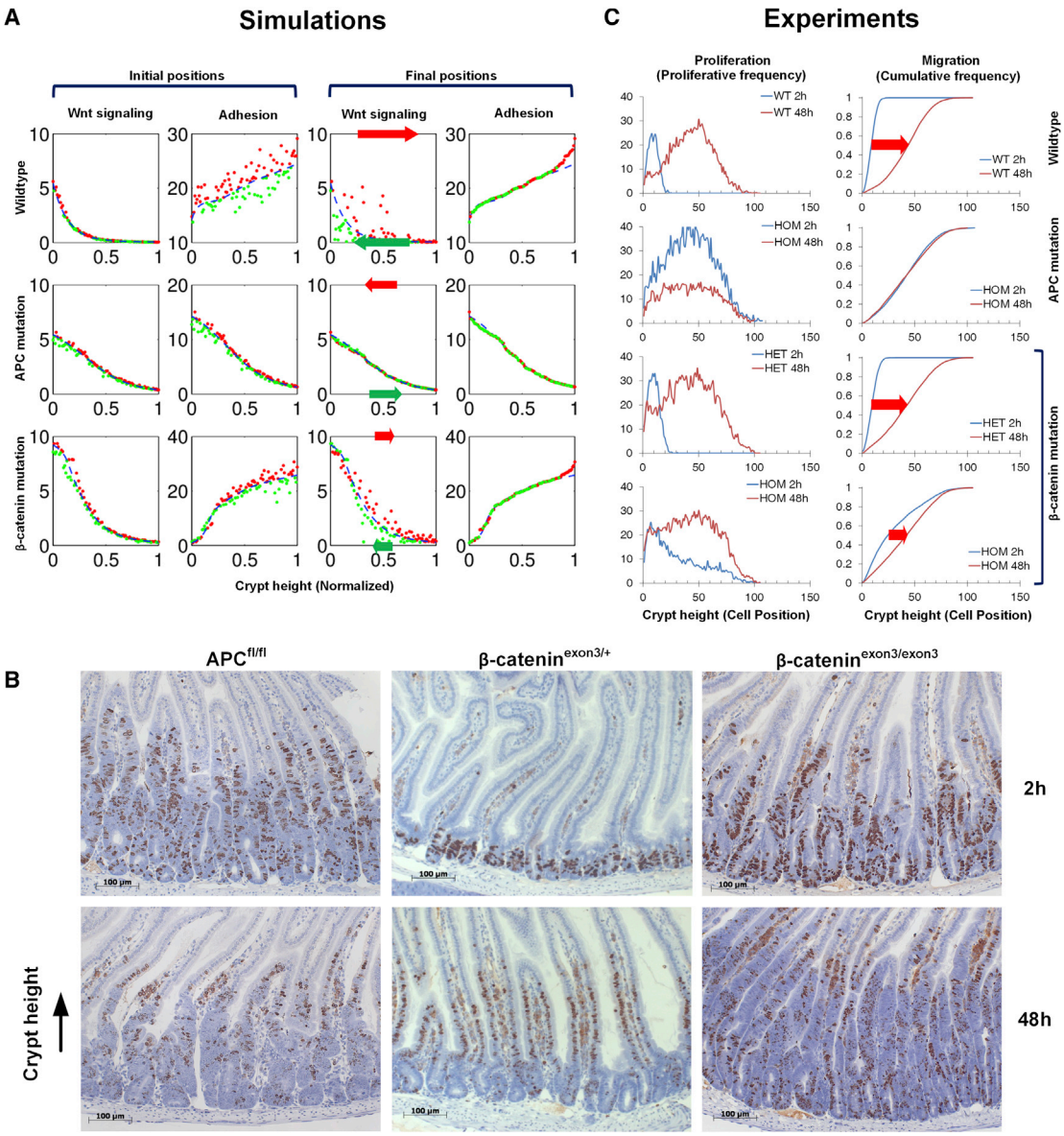


**Figure 5. Experimental Testing of the Model Predictions**

(A) Simulation study investigating the effect of cellular repositioning on the overall heterogeneous cell population in the wild-type crypt (first row), APC mutated crypt (second row), and β-catenin mutated crypt (third row). Here, the heterogeneity was simulated by adding random noise to the noise-free molecular profiles (blue dotted line) for 100 sampled crypt cells (first and second columns). The initial positions of the sampled crypt cells were changed to their final positions after cellular repositioning. Here, we investigated the effect of cellular repositioning on the distribution of Wnt signaling and adhesion (third and fourth columns). Red and green filled circles indicate the positive and negative deviations from the original noise-free molecular profiles. Red and green arrows indicate the migration direction and forces of red and green filled circles, respectively. To test the model predictions, we used in vivo mouse models that have homozygous APC mutation and β-catenin mutation.

(B and C) BrdU-positive cells in 2 hr following BrdU injection are confined to proliferative zones within the crypts in $APC^{fl/fl}$ (homozygous), $\beta\text{-catenin}^{exon3/+}$ (heterozygous), and $\beta\text{-catenin}^{exon3/exon3}$ (homozygous) mutated mice (B, first row). The position of BrdU-positive cells in the crypt axis 48 hr after BrdU injection, indicating migration of labeled cells toward the upper crypt (B, second row). In case of APC mutation, we used the in vivo mouse models that have homozygous mutations (C, second row). In case of β-catenin mutation, we used the in vivo mouse models that have a heterozygous mutation (C, third row) or homozygous mutations (C, fourth row). We monitored BrdU-labeled cells 2 or 48 hr after administrating BrdU as indicated. Because BrdU is incorporated for less than 2 hr postinjection, it gives an indication of the proliferative zone 2 hr postlabeling. At 48 hr, the movement and proliferation of the cells within the crypt can be monitored. We quantified the position and number of proliferative cells (C, left) and then calculated the cumulative frequency (C, right) to measure the cell migration in crypts. Therefore, when the position of the top labeled cells is scored, all events are scored, and hence the cumulative frequency equals 1.0. Arrows in (C) indicate the migration distance of BrdU-labeled cell population. Fifty half-crypts per mouse were scored for at least three different mice per genotype.

See also Tables S3, S4, S5, and S6.

caused by heterogeneous β-catenin expressions. Together, these changes resulted in the migration of cells with a higher proliferative potential toward the bottom of crypt. In our simulations, the average migration distance for cells with a higher (or lower) proliferative potential was −0.04 (0.04, respectively) (see Supplemental Results and Table S4 for details). This means that cells with a higher proliferative potential in the APC mutated crypt will greatly reduce their migration speed (toward top of the crypt) compared to cells with a lower proliferative potential, and thereby they can be accumulated in the crypt. By contrast, the cells with a lower proliferative potential increase their migration speeds (toward top of the crypt), resulting in decreased lifetime in the crypt.

Then, we investigated the effect of β-catenin mutations in stem cells on the repositioning of crypt cells. As APC mutations, β-catenin mutations are an equally important event that can cause colon cancer (Morin et al., 1997), but their incidence is comparatively very rare. It is still unclear why APC mutations are much more frequent than β-catenin mutations, although they both affect the function of the same pathway and should have similar effects when considering the textbook type wiring diagram of this pathway. Therefore, we focused our analysis on the differential effects of β-catenin versus APC mutations (see Supplemental Experimental Procedures for β-catenin mutation). As a result, we found that exon 3 mutations increase Wnt signaling along the crypt. We also found that the fluctuation of Wnt signaling becomes larger (2.67-fold), whereas the fluctuation of adhesion complex formation gets smaller (0.81-fold) compared to wild-type (Supplemental Results; Table S3). These results mean that crypt cells became more proliferative and heterogeneous, when β-catenin was mutated. However, the average migration distance of the cells with a higher proliferative potential toward the upper crypt decreased, because the fluctuation of adhesion became smaller (Figure 5A, third row, Supplemental Results; Table S3). Hence, β-catenin exon 3 mutation increases the chance to initiate cancer. In contrast to when APC is mutated, the β-catenin mutated crypt maintains the same increasing gradient of adhesion as the wild-type (Figure 5A, second column of the third row). Interestingly, the crypt with exon 3 mutation of β-catenin cannot invert the adhesion gradient as the amount of APC increases along the crypt. The inversion of the adhesion gradient facilitates cancer evolution, because it changes the migration direction of cells with a higher proliferative potential and allows them to stay longer in the crypt. From this perspective, the impact of the β-catenin mutation is much weaker than APC mutations. Cells with a higher proliferative potential shift toward upper crypt, but their average migration distance is decreased by 31% compared to the wild-type (Figure 5A, third column of third row; Supplemental Results; Table S4). Taken together, our model predicts that the migration of cells with a higher proliferative potential will be retarded in the β-catenin mutated crypt compared to the wild-type, but the retardation is less efficient than that caused by an APC mutation.

### Experimental Testing of the Model Predictions

To test our model predictions in an animal model, we used genetically engineered mouse models and labeling of cells by injection of 5-bromo-2′-deoxyuridine (BrdU). BrdU is incorporated into replicating DNA (Figure 5B). Because its bioavailability is limited to <2 hr, it marks cells that were proliferating at the time of injection. However, the BrdU label remains in the DNA allowing tracking of the migration of these cells within the crypt. The first mouse model was based on the inducible deletion of APC in the intestinal epithelium (Sansom et al., 2004) (Figure 5C, second row). The second mouse model was an inducible deletion of exon 3 in β-catenin, which contains the GSK-3β phosphorylation sites and hence mimics β-catenin mutations that abolish these phosphorylation sites (Figure 5C, third and fourth rows). Both APC and β-catenin homozygous mutations strongly increased the initial distributions of proliferative frequencies as measured by counting the numbers of BrdU-positive cells 2 hr after BrdU administration (Tables S5and S6; Figure 5C, second and fourth rows). This means that both types of mutated crypts possess cells with a higher proliferative potential compared to the wild-type. We also determined the distribution of BrdU-labeled cells for the APC and the β-catenin models at 48 hr after BrdU administration and compared them to the initial distributions. In case of the APC mutated crypt, the distribution curves (Figure 5C, left of second row) and their cumulative summations (Figure 5C, right of second row) showed no difference of migration between 2 and 48 hr. These data clearly showed that the BrdU-positive cells greatly reduce their migration in the APC mutated crypt. In the case of the β-catenin mutated crypt, homozygous β-catenin mutations decreased the migration of BrdU-positive cells (Figure 5C, fourth row). However, the cumulative summations show that the BrdU-positive cells in β-catenin mutated crypt migrated faster than in the APC mutated crypt. Therefore, the experimental results show a clear agreement with the model predictions about the migration of cells with a high proliferative potential. It may appear contradictory that cells with a higher proliferative potential migrate slower in the in vivo crypt if only the mitotic pressure is considered for the migration (Heath, 1996). Our analysis provides a good explanation why it is not contradictory.

Together, our mathematical simulations combined with in vivo experimental studies show that the increase of crypt cells with a higher proliferative potential and the restructuring of the crypt environment by inverting the adhesion gradient are critical factors for cancer progression in the early stages of colon cancer development.

## DISCUSSION

The critical role of APC and β-catenin mutations in the pathogenesis of CRC is well documented (Fearon, 2011; Najdi et al., 2011; Polakis, 2012; White et al., 2012). However, the molecular mechanistic consequences of these mutations are incompletely understood. Our results highlight the importance of interactions between the subcellular APC network and the adhesion and Wnt gradients in the crypt. The shuttling function of APC coordinates cell adhesion with the transcriptional activity of β-catenin, which induces genes that stimulate proliferation, such as cyclin D and c-Myc (Mosimann et al., 2009; Sansom et al., 2005). Wnt also downregulates E-cadherin expression, thereby exerting a negative feedback on the adhesion pool. This circuitry results in high Wnt responsiveness of the transcriptional function exerted by

the β-catenin:TCF complex, and in high adhesion mediated by high E-cadherin expression when APC function is also high (Figures 2D, 2E, and 2G–2J). However, at low APC levels Wnt selectively stimulated the β-catenin:TCF protein complex and inhibited E-cadherin expression. Thus, loss of APC function differentially affects the formation of the β-catenin signaling and adhesion pools in response to Wnt stimulation favoring the maintenance of the transcriptional function while reducing adhesion. Such changes support the proliferation of mutated cells with enhanced Wnt signaling and compromised APC function. These results are consistent with experimental observations suggesting that the Wnt pathway is activated in two steps during colorectal carcinogenesis, consisting of APC mutation and an additional Wnt stimulation that induces formation of the β-catenin:TCF transcription factor complex (Najdi et al., 2011). They are also consistent with the "just right" hypothesis of Wnt signaling, which is based on mutational studies and work with APC mutants expressed in transgenic mouse models. This hypothesis states that CRC can develop only if Wnt signaling is within an optimal range, and that APC mutations are selected to retain some residual functionality that can satisfy these boundary conditions (Gaspar and Fodde, 2004; Minde et al., 2011; Segditsas and Tomlinson, 2006). A plausible assumption is that such boundary conditions correlate with a major change in APC functionality. In our model, a significant change in APC functionality occurs at the border between zones 1 and 2 (Figures 2D and 2E), where Wnt maintains transcriptional activation but switches from stimulation to suppression of adhesion.

To assess potential biological consequences of such changes in APC functionality in a quantitative manner, we included the microenvironment imposed by the crypt structure into our model. We found that the normal APC expression profile along the crypt axis (i.e., decreasing from top to bottom) is critical to maintain a proper adhesion profile along the crypt that allows cells to migrate up to the top of the crypt and be shed into the lumen. Individual cells adjust their positions to minimize the total sum of the adhesion differences between themselves and their neighbors (Steinberg, 2007). Our simulations showed that this differential adhesion forces in a normal crypt push mutated cells with enhanced Wnt signaling upward, resulting in the elimination of mutant cells. The overall directionality of the adhesion gradient pushing cells upward is preserved as long as APC function is $\geq$50%, which corresponds to a heterozygous situation. Thus, the removal of mutated cells could be maintained for prolonged periods of time, which is consistent with the long latency period between APC mutations and CRC development (Fearon, 2011). However, if APC function in the crypt drops to $\leq$12%, the adhesion gradient reverses allowing mutated cells to stay in the crypt and continue proliferating. Quantitatively, these data fit well with the approximately 10-fold reduction in APC function that marks the border between zones 1 and 2 in Figures 2D and 2E.

Therefore, we conclude that the spatial distribution of APC and formation of an adhesion gradient in the crypt is critical for the tumor suppressor function of APC, and that at the level of an individual cell the coordination between the signaling and adhesion function is quite resilient to the heterozygous loss of APC function.

In summary, our system's biological approach revealed how intracellular signaling, the anatomical structure of the crypt, and adhesion gradients combine to provide a tissue homeostasis strategy that safeguards against tumorigenesis by promoting the removal of mutated and hyperproliferative cells. Although our model captures salient aspects of this homeostasis, it—like any model—is an abstraction that allows us to reduce complex phenomena to reveal underlying principles. The current model is a solid foundation for expansion by considering further aspects such as cell differentiation, apoptosis, and the relationship between mutations in stem cells or transit amplifying cells.

## EXPERIMENTAL PROCEDURES

### Mathematical Modeling

We considered six key molecular species, APC, Axin, β-catenin, TCF, E-cadherin, and Slug, and the extracellular Wnt stimulus as input and employed ordinary differential equations to develop a mathematical model of the molecular interactions (see Supplemental Experimental Procedures for details) (Cho et al., 2003; Cho and Wolkenhauer, 2003). The system equations were numerically integrated using SUNDIALS solvers (https://computation.llnl.gov/casc/sundials/main.html).

### Experimental Testing Using In Vivo Models

All experiments were performed under the UK Home Office guidelines. Outbred mice segregating for the C57BL6J and S129 genomes from 6 to 12 weeks of age were used. The following alleles were used: $Apc^{580Sflox}$ (Sansom et al., 2004), $Catnb^{lox(ex3)}$ (Harada et al., 1999), AhCre (Ireland et al., 2004), AhCreER (Kemp et al., 2004). To induce recombination, mice were given 3 × 80 mg/kg β-naphthoflavone in one single day (AhCre) or 2 × 80 mg/kg/day β-naphthoflavone/tamoxifen for 2 days. Mice were examined 4 days ($AhCre^{+}$ $Apc^{fl/fl}$ 2 hr BrdU), 5 days ($AhCre^{+}$ $Apc^{fl/fl}$ 48 hr BrdU) or 5 days ($AhCreER^{+}$ $Catnb^{lox(ex3)/+}$ and $Catnb^{lox(ex3)/lox(ex3)}$, 2 hr, and 48 hr BrdU) after the first injection. For BrdU labeling, mice were injected either 2 or 48 hr prior to sacrifice with 0.25 ml BrdU (GE Healthcare). The small intestine was harvested and fixed in methacarn (methanol, chloroform, and acetic acid; 4:2:1). Staining for BrdU was performed using an anti-BrdU conjugate (BD Biosciences, 1:200). Cells were counted along the crypt-villus axis from the bottom of the crypt until the last BrdU-positive cell and scored with 0 or 1 for BrdU positivity. At least 50 half-crypts per mouse were scored and three to four mice per genotype. The cumulative frequency was calculated as described previously (Sansom et al., 2004). The detailed scoring data can be found in Tables S5 and S6.

## SUPPLEMENTAL INFORMATION

Supplemental Information includes Supplemental Experimental Procedures, Supplemental Results, four figures, and six tables and can be found with this article online at http://dx.doi.org/10.1016/j.celrep.2014.02.043.

## ACKNOWLEDGMENTS

The authors thank Dongkwan Shin and Tae-Hwan Kim for their helpful discussion. This work was supported by the National Research Foundation of Korea (NRF) grants funded by the Korean Government, the Ministry of Science, ICT & Future Planning (2010-0017662). W.K. acknowledges the support by the Science Foundation Ireland under grant no. 06/CE/B1129. O.J.S. acknowledges the support received from a CrUK core grant and an ERC starter grant "Coloncan." D.J.H. is supported by the EU FP7 grant no. 278568 "PRIMES."

Received: July 30, 2013
Revised: February 3, 2014
Accepted: February 26, 2014
Published: March 27, 2014

## REFERENCES

Azcárate-Peril, M.A., Sikes, M., and Bruno-Bárcena, J.M. (2011). The intestinal microbiota, gastrointestinal environment and colorectal cancer: A putative role for probiotics in prevention of colorectal cancer? Am. J. Physiol. *301*, G401–G424.

Brabletz, T., Jung, A., Hermann, K., Günther, K., Hohenberger, W., and Kirchner, T. (1998). Nuclear overexpression of the oncoprotein beta-catenin in colorectal cancer is localized predominantly at the invasion front. Pathol. Res. Pract. *194*, 701–704.

Cho, K.H., and Wolkenhauer, O. (2003). Analysis and modelling of signal transduction pathways in systems biology. Biochem. Soc. Trans. *31*, 1503–1509.

Cho, K.-H., Shin, S.-Y., Lee, H.-W., and Wolkenhauer, O. (2003). Investigations into the analysis and modeling of the TNF alpha-mediated NF-kappa B-signaling pathway. Genome Res. *13*, 2413–2422.

Cho, K.-H., Baek, S., and Sung, M.-H. (2006). Wnt pathway mutations selected by optimal beta-catenin signaling for tumorigenesis. FEBS Lett. *580*, 3665–3670.

Davies, P.S., Dismuke, A.D., Powell, A.E., Carroll, K.H., and Wong, M.H. (2008). Wnt-reporter expression pattern in the mouse intestine during homeostasis. BMC Gastroenterol. *8*, 57.

Diggs, D.L., Huderson, A.C., Harris, K.L., Myers, J.N., Banks, L.D., Rekhadevi, P.V., Niaz, M.S., and Ramesh, A. (2011). Polycyclic aromatic hydrocarbons and digestive tract cancers: a perspective. J Environ Sci Health C Environ Carcinog Ecotoxicol Rev *29*, 324–357.

Fearon, E.R. (2011). Molecular genetics of colorectal cancer. Annu. Rev. Pathol. *6*, 479–507.

Ferlay, J., Shin, H.R., Bray, F., Forman, D., Mathers, C., and Parkin, D.M. (2010). GLOBOCAN 2008 v1.2: Cancer Incidence and Mortality Worldwide: IARC CancerBase No. 10. Lyon (France): IARC Press. http://globocan.iarc.fr.

Fodde, R., Smits, R., and Clevers, H. (2001). APC, signal transduction and genetic instability in colorectal cancer. Nat. Rev. Cancer *1*, 55–67.

Gaspar, C., and Fodde, R. (2004). APC dosage effects in tumorigenesis and stem cell differentiation. Int. J. Dev. Biol. *48*, 377–386.

Gatenby, R.A., Gillies, R.J., and Brown, J.S. (2010). Evolutionary dynamics of cancer prevention. Nat. Rev. Cancer *10*, 526–527.

Harada, N., Tamai, Y., Ishikawa, T., Sauer, B., Takaku, K., Oshima, M., and Taketo, M.M. (1999). Intestinal polyposis in mice with a dominant stable mutation of the beta-catenin gene. EMBO J. *18*, 5931–5942.

Heath, J.P. (1996). Epithelial cell migration in the intestine. Cell Biol. Int. *20*, 139–146.

Herzig, M., Savarese, F., Novatchkova, M., Semb, H., and Christofori, G. (2007). Tumor progression induced by the loss of E-cadherin independent of β-catenin/Tcf-mediated Wnt signaling. Oncogene *26*, 2290–2298.

Humphries, A., and Wright, N.A. (2008). Colonic crypt organization and tumorigenesis. Nat. Rev. Cancer *8*, 415–424.

Ireland, H., Kemp, R., Houghton, C., Howard, L., Clarke, A.R., Sansom, O.J., and Winton, D.J. (2004). Inducible Cre-mediated control of gene expression in the murine gastrointestinal tract: effect of loss of β-catenin. Gastroenterology *126*, 1236–1246.

Kemp, R., Ireland, H., Clayton, E., Houghton, C., Howard, L., and Winton, D.J. (2004). Elimination of background recombination: somatic induction of Cre by combined transcriptional regulation and hormone binding affinity. Nucleic Acids Res. *32*, e92.

Minde, D.P., Anvarian, Z., Rüdiger, S.G., and Maurice, M.M. (2011). Messing up disorder: how do missense mutations in the tumor suppressor protein APC lead to cancer? Mol. Cancer *10*, 101–101.

Morin, P.J., Sparks, A.B., Korinek, V., Barker, N., Clevers, H., Vogelstein, B., and Kinzler, K.W. (1997). Activation of β-catenin-Tcf signaling in colon cancer by mutations in β-catenin or APC. Science *275*, 1787–1790.

Mosimann, C., Hausmann, G., and Basler, K. (2009). Beta-catenin hits chromatin: regulation of Wnt target gene activation. Nat. Rev. Mol. Cell Biol. *10*, 276–286.

Murray, P.J., Kang, J.-W., Mirams, G.R., Shin, S.-Y., Byrne, H.M., Maini, P.K., and Cho, K.-H. (2010). Modelling spatially regulated beta-catenin dynamics and invasion in intestinal crypts. Biophys. J. *99*, 716–725.

Muzny, D.M., Bainbridge, M.N., Chang, K., Dinh, H.H., Drummond, J.A., Fowler, G., Kovar, C.L., Lewis, L.R., Morgan, M.B., Newsham, I.F., et al.; Cancer Genome Atlas Network (2012). Comprehensive molecular characterization of human colon and rectal cancer. Nature *487*, 330–337.

Najdi, R., Holcombe, R.F., and Waterman, M.L. (2011). Wnt signaling and colon carcinogenesis: beyond APC. J. Carcinog. *10*, 5.

Nowak, M.A., Michor, F., and Iwasa, Y. (2003). The linear process of somatic evolution. Proc. Natl. Acad. Sci. USA *100*, 14966–14969.

Okamoto, R., and Watanabe, M. (2004). Molecular and clinical basis for the regeneration of human gastrointestinal epithelia. J. Gastroenterol. *39*, 1–6.

Pearson, J.R., Gill, C.I., and Rowland, I.R. (2009). Diet, fecal water, and colon cancer—development of a biomarker. Nutr. Rev. *67*, 509–526.

Phelps, R.A., Broadbent, T.J., Stafforini, D.M., and Jones, D.A. (2009). New perspectives on APC control of cell fate and proliferation in colorectal cancer. Cell Cycle *8*, 2549–2556.

Polakis, P. (2012). Drugging Wnt signalling in cancer. EMBO J. *31*, 2737–2746.

Powell, S.M., Zilz, N., Beazer-Barclay, Y., Bryan, T.M., Hamilton, S.R., Thibodeau, S.N., Vogelstein, B., and Kinzler, K.W. (1992). APC mutations occur early during colorectal tumorigenesis. Nature *359*, 235–237.

Sansom, O.J., Reed, K.R., Hayes, A.J., Ireland, H., Brinkmann, H., Newton, I.P., Batlle, E., Simon-Assmann, P., Clevers, H., Nathke, I.S., et al. (2004). Loss of Apc in vivo immediately perturbs Wnt signaling, differentiation, and migration. Genes Dev. *18*, 1385–1390.

Sansom, O.J., Reed, K.R., van de Wetering, M., Muncan, V., Winton, D.J., Clevers, H., and Clarke, A.R. (2005). Cyclin D1 is not an immediate target of beta-catenin following Apc loss in the intestine. J. Biol. Chem. *280*, 28463–28467.

Segditsas, S., and Tomlinson, I. (2006). Colorectal cancer and genetic alterations in the Wnt pathway. Oncogene *25*, 7531–7537.

Steinberg, M.S. (2007). Differential adhesion in morphogenesis: a modern view. Curr. Opin. Genet. Dev. *17*, 281–286.

van de Wetering, M., Sancho, E., Verweij, C., de Lau, W., Oving, I., Hurlstone, A., van der Horn, K., Batlle, E., Coudreuse, D., Haramis, A.P., et al. (2002). The beta-catenin/TCF-4 complex imposes a crypt progenitor phenotype on colorectal cancer cells. Cell *111*, 241–250.

White, B.D., Chien, A.J., and Dawson, D.W. (2012). Dysregulation of Wnt/β-catenin signaling in gastrointestinal cancers. Gastroenterology *142*, 219–232.

# The APC network regulates the removal of mutated cells from colonic crypts

Je-Hoon Song[1], David J. Huels[2], Rachel A. Ridgway[2], Owen J. Sansom[2], Boris N. Kholodenko[3,4,5], Walter Kolch[3,4,5], and Kwang-Hyun Cho[1*]

[1]Department of Bio and Brain Engineering, Korea Advanced Institute of Science and Technology (KAIST), 291 Daehak-ro, Yuseong-gu, Daejeon 305-701, Republic of Korea.

[2]The Beatson Institute for Cancer Research, Garscube Estate, Glasgow G61 1BD, U.K.

[3]Systems Biology Ireland, University College Dublin, Belfield, Dublin 4, Ireland.

[4]Conway Institute of Biomolecular and Biomedical Research, University College Dublin, Belfield, Dublin 4, Ireland.

[5]School of Medicine and Medical Science, University College Dublin, Belfield, Dublin 4, Ireland.

# Supplemental Information

[*]Corresponding author, E-mail: ckh@kaist.ac.kr, Phone: +82-42-350-4325, Fax: +82-42-350-4310, Web address: http://sbie.kaist.ac.kr

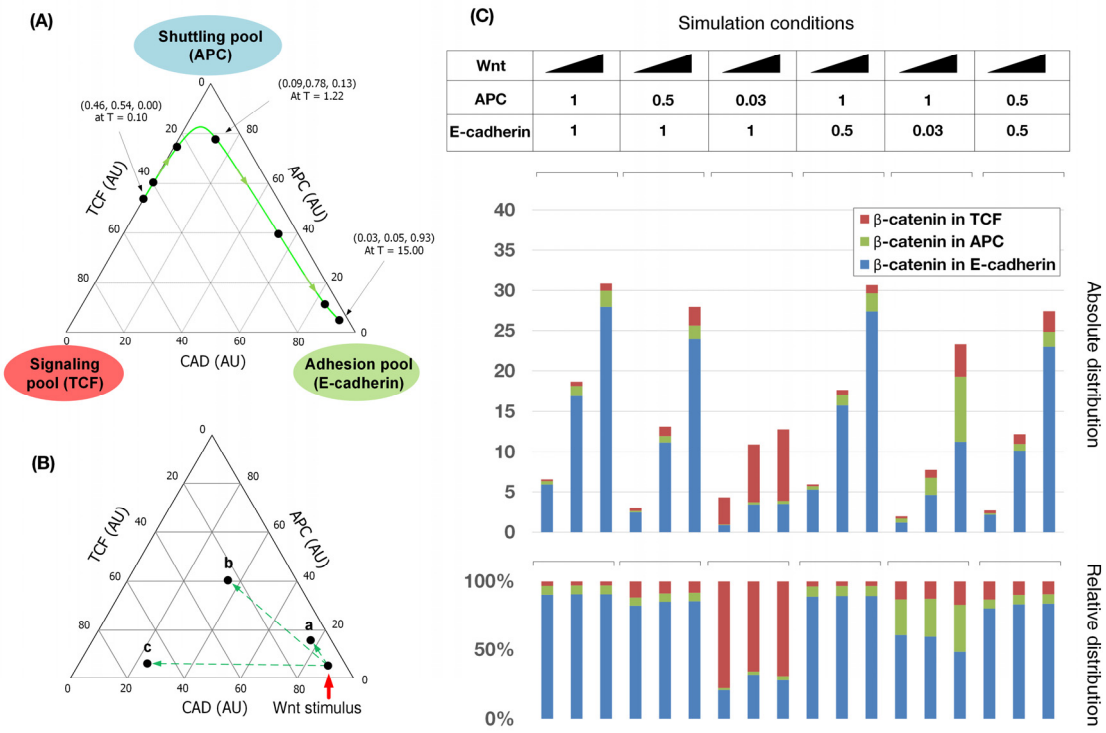


**Figure S1. Analysis of the dynamic distribution of β-catenin into its different functional complexes, Related to Figure 2.** (**A**) The dynamic behaviour described in Figure 2C was analyzed using ternary plots. In this plot a ternary state is determined by the relative ratios of signaling ($S_S$), adhesion ($S_A$), and shuttling ($S_T$) pools. The state trajectory shows that there is a strong flow of β-catenin from the signaling pool via the shuttling pool to the adhesion pool. This ternary state reached a steady state in 15 hours. (**B**) The steady state of (A) was perturbed by Wnt stimulation under the condition of (a) wildtype E-cadherin and APC expression, (b) E-cadherin knock down, and (c) APC knock down, respectively. In case of wildtype conditions the steady state was robustly maintained and the ternary state only modestly shifted towards the upper corner, which means that APC effectively absorbed the surplus β-catenin accumulation induced by Wnt stimulation. Comparing (b) and (c) indicates that APC repression is a more effective way to increase the Wnt sensitivity in terms of transcriptional signaling. (**C**) Absolute values (upper stacked column graph) and normalized values (lower stacked column graph) of the distribution ratio of β-catenin under combinational knock down of E-cadherin and APC. Coinciding with the ternary plot (B), APC knock down is more effective than E-cadherin knock down.

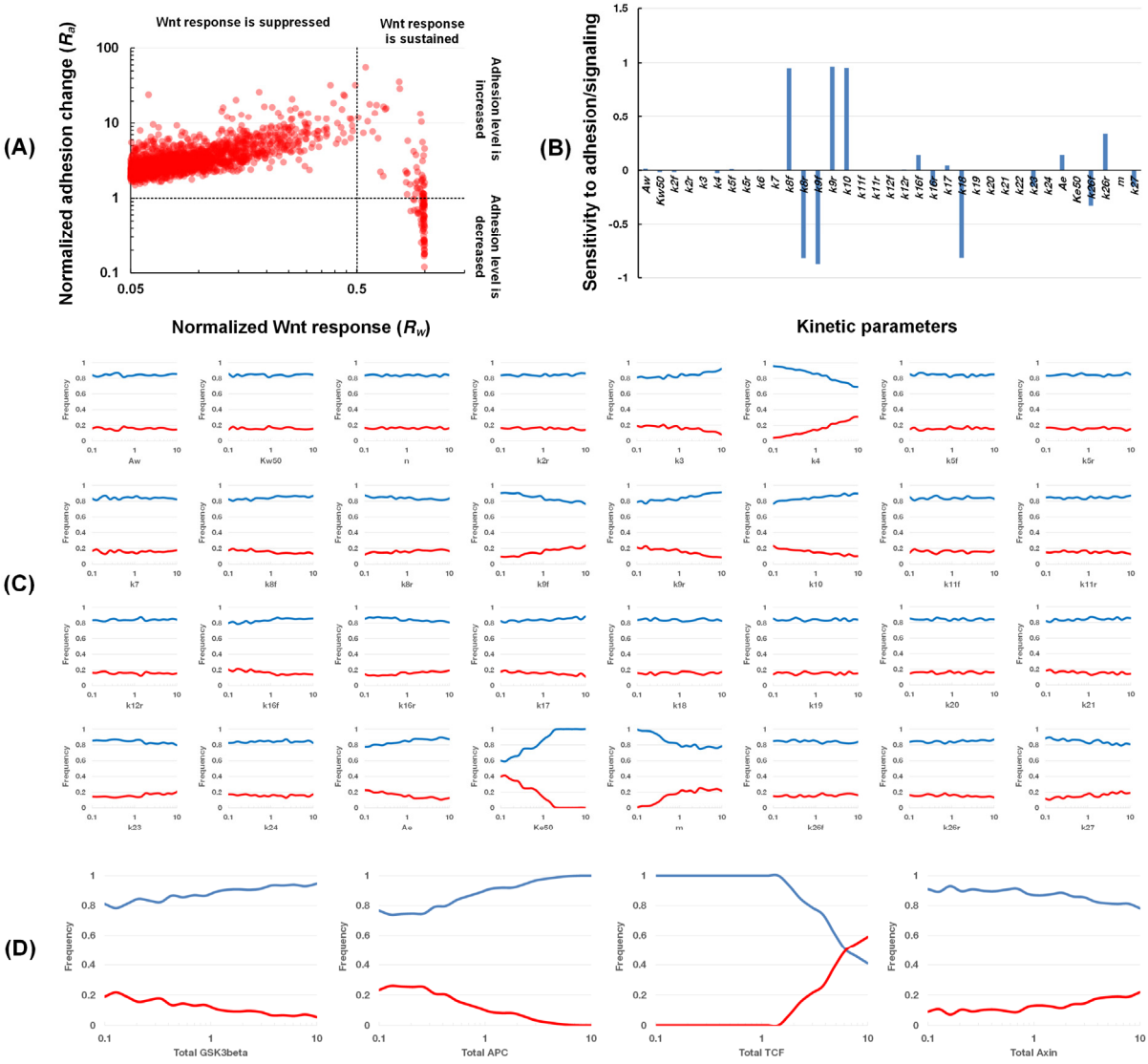


**Figure S2. Parameter screening and sensitivity analysis for the mathematical model, Related to Figure 2 and Parameter Optimization and Screening.** (**A**) Scatter plot for optimized parameter sets. As the set of parameter values of the mathematical model is not uniquely determined, the parameter values were repeatedly estimated to obtain a population of the sets of parameter values (the number of parameter sets, $S_1$ = 1840). We estimated model parameters that fit both the time-series measurements from E-cadherin-free cell line and the E-cadherin expression levels (step 1 in the parameter estimation). In order to understand the common dynamical behavior of the mathematical model for the parameter population ($S_1$), we investigated the normalized Wnt responses and the normalized adhesion changes from the scatter

plot. A normalized Wnt response ($R_w$) is defined by the Wnt activation level (β-catenin:TCF) divided by the Wnt activation level under E-cadherin-free condition. A normalized adhesion change ($R_a$) is defined by the adhesion level (β-catenin:E-cadherin) in response to Wnt stimulus normalized with respect to the basal adhesion level. We presented the pairs of $R_w$ and $R_a$ on the scatter plot as *x*- and *y*-axis, respectively. The population of these parameter estimates showed a bimodal distribution of Wnt responses where one group of parameter sets have high Wnt responses ($R_w > 0.5$) whereas the other group of parameter sets have low Wnt responses ($R_w < 0.5$). Such a bimodal distribution is caused by the mutual inhibitory structure of the integrated subcellular network, where E-cadherin inhibits Wnt signaling by sequestering β-catenin from TCF and Wnt signaling inhibits E-cadherin expression via transcriptional regulation (Figure 1B). For the parameter sets in the sustained region, the Wnt response ($R_w$) was not significantly changed even when E-cadherin was expressed, and the adhesion can be reduced by Wnt stimulus. In the suppressed region, by contrast, Wnt responses ($R_w$) were significantly reduced and the adhesion levels were increased by Wnt stimulus. (**B**) Local sensitivity analysis. Local sensitivity of the mathematical model was investigated, where the output of the system was considered as the ratio of adhesion to signaling level at steady state. Local sensitivity analysis shows the robustness of the subcellular distribution of β-catenin in the signaling and adhesion pools with respect to the perturbation of kinetic parameters. (**C** and **D**) Global sensitivity analysis (GSA) of the mathematical model. For each kinetic parameter (C) and protein abundance (D), a parameter space was randomly generated within a given range (from 0.1 to 10 fold of the reference parameters). Objective function for GSA is defined such that it returns 1 (or acceptable) if additional β-catenin increases the adhesion level or it returns -1 (or unacceptable) if additional β-catenin decreases the adhesion level. For each parameter, the frequency of 'acceptable' or 'unacceptable' is presented with blue or red line, respectively.

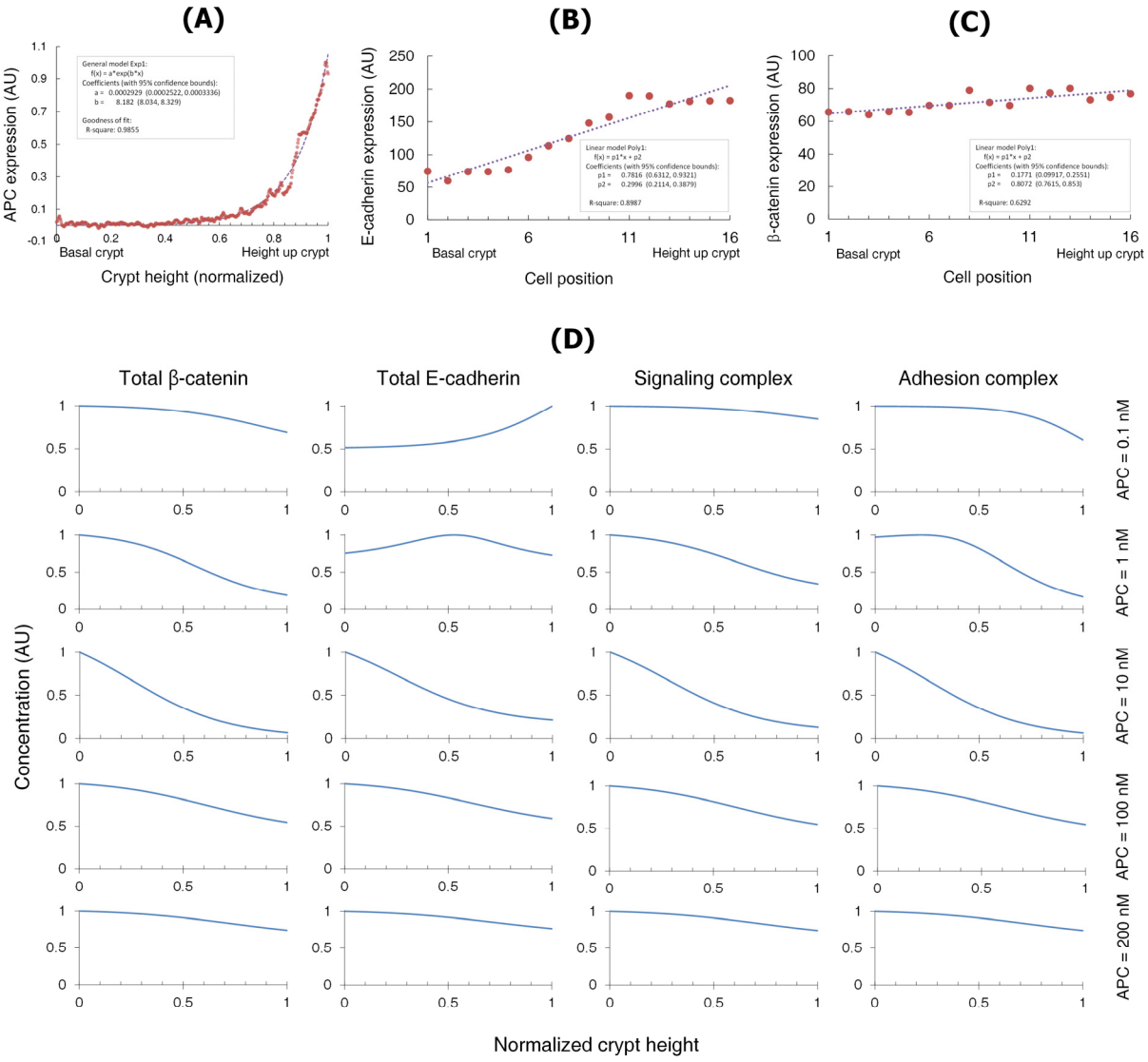


**Figure S3. The gradient of APC expression plays an important role in defining the direction of the adhesion gradient along the crypt, Related to Figure 3.** (**A**) APC expression level increases along the crypt. Immunostaining analysis performed by Senda et al. shows that APC expression has increasing profile along the crypt (Senda et al., 2007). The quantified data from the experimental image fits to exponential function. (**B** and **C**) Characteristic molecular profiles measured from *in vivo* experiments. The qualitative profiles of E-cadherin and β-catenin were used to estimate the parameters of the mathematical model. E-cadherin was increased (B) and β-catenin (C) was increased along the crypt. Numerical data were taken from (Escaffit et al., 2005).

(**D**) Reproduced molecular profiles along the crypt by simulating the IMC model with constant APC expression profiles. Instead of the gradient APC expression profile, a constant profile of $APC_{Total}(x)$ (200, 100, 10, 1, and 0.1 nM) was used to simulate the IMC model. Constant expression profiles of APC cannot explain the experimental observation of an increasing β-catenin profile along the crypt. This subsequently fails to establish the increasing gradient of adhesion towards the top of the crypt, although the formation of the signaling complex exhibits a decreasing profile in accord with experimental observations. These results show that the gradient of APC expression plays an important role in defining the direction of the adhesion gradient along the crypt.

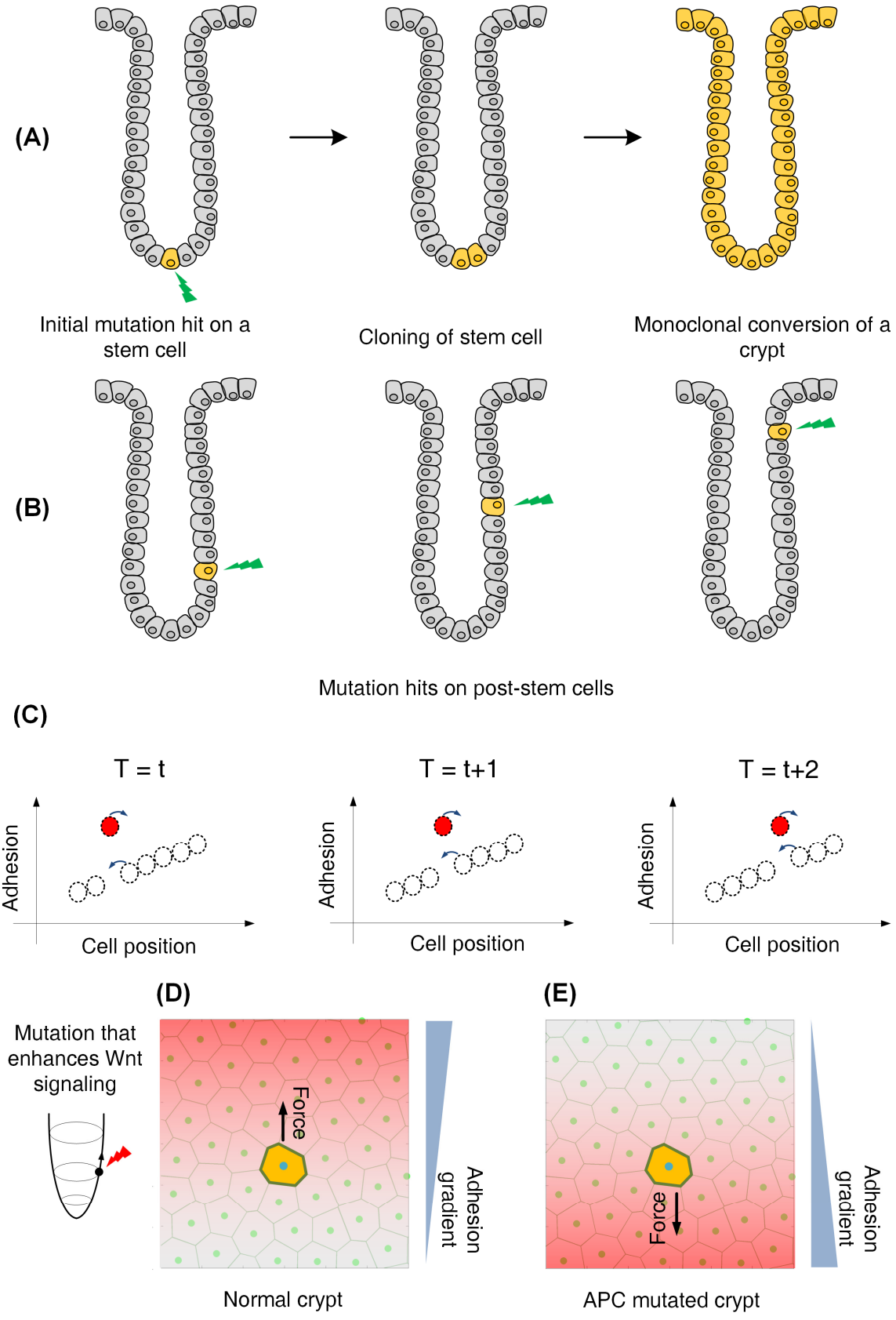
(A)
Initial mutation hit on a stem cell
Cloning of stem cell
Monoclonal conversion of a crypt
(B)
Mutation hits on post-stem cells
(C)
T = t
T = t+1
T = t+2
Adhesion
Cell position
(D)
Mutation that enhances Wnt signaling
Force
Adhesion gradient
Normal crypt
(E)
Force
Adhesion gradient
APC mutated crypt

**Figure S4. Schematic illustration of the mutation models and the suggested model for crypt homeostasis, Related to Figure 4.** (**A**,**B**) Schematic illustration of the two mutation models. (A) Mutations that hit a stem cell cause the monoclonal conversion of a crypt. (B) Mutations occurring in the post-stem cell compartment affect cells at different heights of a crypt. To investigate the effects of mutations on the crypt, we considered stem cell mutations and somatic cell mutations. A stem cell clone with mutations expands towards upper crypt, thereby the progeny of a mutant stem cell eventually replaces all other cells in the crypt (A) (Humphries and Wright, 2008). This means that the mutations of a stem cell can change the signaling and adhesion molecular profiles in the IMC model. By contrast, the effects of somatic mutations were considered as local perturbations in a normal crypt or in a mutated crypt with stem cell mutation (B). (**C**-**E**) Schematic illustration of cell position and crypt homeostasis. (C) Illustration of the cell migration process guided by the adhesion gradient. The mutated cell (red) with additional β-catenin shows enhanced adhesion, thereby the cell position is reconfigured to minimize adhesion difference. (D) Normal crypt cells direct mutated cells with enhanced Wnt signaling towards the top of the crypt to be shed. (E) In an APC mutated crypt the adhesion gradient can become reversed resulting in the retention of mutated cells.

**Table S1. Parameter estimates for the molecular interaction network, Related to Parameter Optimization and Screening.**

| Symbol | Unit | Value | Symbol | Unit | Value |
|---|---|---|---|---|---|
| $A_w$ | - | 1.48E+02 | $k_{12r}$ | $\text{min}^{-1}$ | 2.56E+03 |
| $k_{2f}$ | $\text{nmol}^{-1} \cdot \text{min}^{-1}$ | 3.45E-03 | $k_{16f}$ | $\text{nmol}^{-1} \cdot \text{min}^{-1}$ | 5.84E+00 |
| $k_{2r}$ | $\text{min}^{-1}$ | 1.85E-05 | $k_{16r}$ | $\text{min}^{-1}$ | 7.51E+00 |
| $k_3$ | $\text{min}^{-1}$ | 1.83E-01 | $k_{17}$ | $\text{min}^{-1}$ | 4.32E-01 |
| $k_4$ | $\text{nmol} \cdot \text{min}^{-1}$ | 1.38E+01 | $k_{18}$ | $\text{min}^{-1}$ | 4.62E-02 |
| $k_{5f}$ | $\text{nmol}^{-1} \cdot \text{min}^{-1}$ | 2.54E+00 | $k_{19}$ | $\text{min}^{-1}$ | 9.48E+00 |
| $k_{5r}$ | $\text{min}^{-1}$ | 5.01E+02 | $k_{20}$ | $\text{min}^{-1}$ | 1.40E+00 |
| $k_6$ | $\text{min}^{-1}$ | 1.67E+03 | $k_{21}$ | $\text{min}^{-1}$ | 9.26E+01 |
| $k_7$ | $\text{min}^{-1}$ | 1.94E+04 | $k_{22}$ | $\text{min}^{-1}$ | 2.25E+00 |
| $k_{8f}$ | $\text{nmol}^{-1} \cdot \text{min}^{-1}$ | 7.89E+00 | $k_{23}$ | $\text{min}^{-1}$ | 2.02E+00 |
| $k_{8r}$ | $\text{min}^{-1}$ | 1.17E+02 | $k_{24}$ | - | 1.23E+04 |
| $k_{9f}$ | $\text{nmol}^{-1} \cdot \text{min}^{-1}$ | 5.22E+00 | $A_E$ | - | 5.75E+01 |
| $k_{9r}$ | $\text{min}^{-1}$ | 2.26E+02 | $K_{e50}$ | - | 7.61E+00 |
| $k_{10}$ | $\text{min}^{-1}$ | 7.20E+00 | $m$ | - | 8.18E+00 |
| $k_{11f}$ | $\text{nmol}^{-1} \cdot \text{min}^{-1}$ | 4.99E+01 | $k_{26f}$ | - | 1.22E+00 |
| $k_{11r}$ | $\text{min}^{-1}$ | 5.90E+02 | $k_{26r}$ | - | 6.43E+00 |
| $k_{12f}$ | $\text{min}^{-1}$ | 1.83E+01 | $k_{27}$ | - | 1.59E+00 |

**Table S2. E-cadherin expression levels obtained from the mathematical model and experiments, Related to Parameter optimization and screening.**

| Type | Estimated value (nM) | Experimental value (nM) | Average value (nM) | Reference |
|---|---|---|---|---|
| Surface E-cadherin | 38.14 | 23.7 – 158 | 91 | (Duguay et al., 2003; Moran et al., 2010) |
| Internalized E-cadherin | 19.7 | 5.2 – 34.7† | 20† | (Le et al., 1999) |
| Total E-cadherin | 57.84 | 28.9 – 192.7‡ | 111‡ | - |

(†) The numerical data were inferred from the experiment performed by Le et al (Le et al., 1999). (‡) Experimental value of total E-cadherin was inferred by adding surface E-cadherin to internalized E-cadherin.

**Table S3. Statistics showing the influences on signaling and adhesion in the heterogeneous cell population (for the first and second columns of Figure 5A).**

| | Variation in signaling (a relative ratio w.r.t. the wild type) | Variation in adhesion (a relative ratio w.r.t. the wild type) | Ratio of variations for adhesion and signaling |
|---|---|---|---|
| WT | 0.11 (1) | 2.05 (1) | 18.55 |
| APC mutation | 0.21 (1.86) | 0.64 (0.31) | 3.11 |
| β-catenin mutation | 0.29 (2.67) | 1.67 (0.81) | 5.67 |

In order to investigate the endogenous heterogeneity of crypt cells, we considered a set of cells evenly sampled along the crypt that has the decreasing profile of Wnt signaling (β-catenin:TCF) and the increasing profile of E-cadherin-mediated adhesion (E-cadherin:β-catenin) along with the upper direction of the crypt. Initially, the adhesion levels of the sampled cells along the crypt are monotonically increasing (Figure 5A, blue dashed line of 2nd column). Therefore, cells have minimal differences of adhesion to their neighbors. This means the net migration for each crypt cell caused by adhesion difference is zero. Then, random noise with standard deviation ($\sigma = 0.2$) is added to the *de novo* synthesis rate of β-catenin ($k_4$) to simulate the heterogeneous β-catenin expression. Such noise causes variations in both Wnt signaling and E-cadherin-mediated adhesion (1st and 2nd columns in Figure 5A, and Table S3), and thereby disturbs the minimized sum of differential adhesion for crypt cells.

Since E-cadherin-mediated adhesion and Wnt signaling have correlation in the model, repositioning of cells according to the adhesion level significantly affects the distribution of the levels of Wnt signaling along the crypt. We marked the initial positions of the cells with red and green filled circle (Figure 5A, 1st and 2nd columns). The red (green) filled circles mean cells with a higher (a lower, respectively) proliferative potential. The initial positions of the cells are

repositioned according to the level of adhesion in each crypt cell and the repositioning is calculated by using numerical sorting algorithm (Figure 5A, 3rd and 4th columns). The migration distance of each crypt cell is measured by tracing the final position after repositioning (Figure 5A, 3rd column). Cellular positions and average migration distances are summarized (Table S4). $N_{w+}$ ($N_{w-}$) indicates the number of cells that show more (less) Wnt signaling. $N_{w+,in}$ ($N_{w+,out}$) indicates the increase in the number of Wnt cells that migrate towards upper (lower) crypt. $N_{w-,in}$ ($N_{w-,out}$) indicates the decrease in the number of Wnt cells that migrate toward upper (lower) crypt. $M$ indicates the average migration distance. Yellow box denotes the dominant directions of migration where positive (negative) values imply that most cells migrate toward upper (lower) crypt.

**Table S4. Summary of the data in Figure 5A.**

| | $N_{w+}$ | $N_{w-}$ | $N_{w+,in}$ | $N_{w+,out}$ | $N_{w-,in}$ | $N_{w-,out}$ | $M_{w+,in}$ | $M_{w+,out}$ | $M_{w-,in}$ | $M_{w-,out}$ |
|---|---|---|---|---|---|---|---|---|---|---|
| WT | 52 | 48 | 1 | 51 | 44 | 4 | -0.03 | 0.13 | -0.15 | 0.01 |
| APC mutation | 47 | 53 | 43 | 4 | 2 | 51 | -0.04 | 0.01 | -0.02 | 0.04 |
| β-catenin mutation | 51 | 49 | 10 | 41 | 30 | 19 | -0.02 | 0.09 | -0.12 | 0.01 |

**Table S5. BrDU scoring data for APC mutated crypt, Related to Figure 5.** The numerical data presented in the file were used to analyze the frequency and cumulative frequency of proliferation in Figure 5(C, 2nd row).

**Table S6. BrDU scoring data for wildtype crypt and β-catenin mutated crypt, Related to Figure 5.** The numerical data presented in the file were used to analyze the frequency and cumulative frequency of proliferation in Figure 5(C, 1, 3, and 4th rows).

# SUPPLEMENTAL RESULTS

## Construction of a mathematical model for the dynamic analysis of multiple β-catenin functions

In order to study the dual role of β-catenin as component of the Wnt signaling pathway and E-cadherin adhesion systems (Figure 1A) we developed a mathematical model (Figure 1B) that allowed us to investigate the dynamics of (i) the Wnt signaling pathway and resulting suppression of E-cadherin transcription; (ii) the formation of functional E-cadherin - β-catenin adhesion complexes at the cell membrane; (iii) the removal and recycling of E-cadherin - β-catenin adhesion complexes by endocytosis; and (iv) the role of APC in coordinating the participation of β-catenin in adhesion vs. Wnt signaling. The concept of this coordination can be described in a simplified scheme as dynamic distribution of β-catenin between three distinct compartments: a signaling pool in the cytosol and nucleus, an adhesion pool in association with E-cadherin at the cell membrane, and a shuttling pool where APC actively delivers β-catenin to the cell membrane (Figure 1C). The model was constructed and parameterized based on experimental data (for details see Tables S1,S2).

Briefly, the model is based on the following experimental findings: (E1) β-catenin levels are controlled by the destruction complex, which degrades β-catenin and itself is negatively controlled by Wnt signaling (MacDonald et al., 2009); (E2) E-cadherin significantly represses the signaling function of β-catenin at endogenous (Kuphal and Behrens, 2006) as well as artificially controlled levels (Herzig et al., 2007); (E3) Stabilization of β-catenin increases β-catenin:E-cadherin complex formation, and thereby enhances cellular adhesion in various cell types (Bradley et al., 1993; Hinck et al., 1994; Papkoff et al., 1996; Toyofuku et al., 2000). (E4)

The β-catenin:E-cadherin complex can be endocytosed with dissociation and degradation of the components in the cytosol (Fujita et al., 2002; Pece and Gutkind, 2002). E-cadherin can be recycled back to the membrane (Le et al., 1999); (E5) At the same time, the signaling function of β-catenin in the Wnt pathway represses E-cadherin expression by inducing transcription of its inhibitor Slug (Conacci-Sorrell et al., 2003); (E6) Wildtype APC promotes cellular adhesion (Faux et al., 2004), and APC mutations compromise both cell adhesion and migration as shown in *Drosophila* and mammalian cells (Bienz and Hamada, 2004; Hamada and Bienz, 2002; Klingelhöfer et al., 2003); (E7) β-catenin has a shared interaction interface that significantly overlaps between binding partners (Bienz and Clevers, 2003) suggesting mutually exclusive and competitive interactions with different binding proteins. Indeed, competitive binding between APC vs. TCF, APC vs. E-cadherin, and TCF vs. E-cadherin was observed (Hülsken et al., 1994; Neufeld et al., 2000; Orsulic et al., 1999; Rubinfeld et al., 1995); (E8) APC is a highly mobile protein that shuttles continuously between the distinct subcellular pools. Bienz et al. suggested the 'APC shuttling' as delivery mechanism where APC protein picks up β-catenin in the cytosolic signaling pool and delivers it to the adhesion pool at the membrane (Figure 1C) (Bienz, 1999; Bienz and Hamada, 2004; Hamada and Bienz, 2002). APC and APC-β-catenin complexes are transported along microtubules from the cytoplasm towards membrane protrusions (Jimbo et al., 2002). Based on these observations, our model assumes that APC actively transports β-catenin from the cytosol to the membrane, and that the APC - β-catenin complex in the membrane can dissociate and that free subunits can diffuse back to the cytoplasm.

In addition, we also considered spatial influences exerted on cells by their position in the crypt due to the gradients of Wnt, Wnt signaling, APC and E-cadherin expression along the crypt axis (Figure 1D). Wnt expression and Wnt activated signaling as measured by reporter gene

activation decrease towards the top of the crypt (Fevr et al., 2007; Gaspar and Fodde, 2004; van de Wetering et al., 2002). By contrast, the expression of E-cadherin at the cell membrane (Escaffit et al., 2005) and APC expression increase from bottom to top of the crypt (Aust et al., 2001; Fodde et al., 2001; Gaspar and Fodde, 2004; Long et al., 2011; Midgley et al., 1997; Senda et al., 2007; Smith et al., 1993). Information regarding a β-catenin expression gradient along the crypt axis is controversial, with reports claiming a decrease towards the top (Anderson et al., 2002; Batlle et al., 2002) or no change throughout the crypt axis (Aust et al., 2001; Escaffit et al., 2005; Iwamoto et al., 2000). However, all reports agree that cells with nuclear β-catenin are enriched at the bottom of the crypts reflecting a higher transcripional activity of the Wnt pathway in the proliferative compartement of the crypt.

**Model analysis reveals hidden dynamic regulatory principles of β-catenin functions**

Using the mathematical model, we analyzed the hypothesis that the functions of β-catenin in adhesion or Wnt signaling are mutually exclusive and determined by dynamic changes in β-catenin protein interactions. In order to assess the performance of the model we first simulated the effect of Wnt stimulation on β-catenin stabilization and compared it to experimental data (Figure 2A). The experimental data were taken from a quantitative analysis of β-catenin accumulation over a timecourse of Wnt stimulation of L-cells (Hannoush, 2008). As L-cells lack E-cadherin expression (Nagafuchi et al., 1987), the rate of *de novo* E-cadherin synthesis (parameter $A_E$) was set to zero. The increase in the total amount of β-catenin predicted by the model corresponded well to the experimentally measured timecourse profile of β-catenin levels in response to four different Wnt concentrations (Figure 2A). At steady state, the β-catenin:TCF signaling complex in response to Wnt (400ng/ml) was also highly abundant when $A_E$ was

decreased 10 fold (Figure 2B). Increasing E-cadherin expression by increasing $A_E$ decreased the β-catenin:TCF signaling complex with switch-like kinetics, which results from the mutual inhibition of the signaling complex and E-cadherin. The β-catenin:TCF signaling complex inhibits E-cadherin expression by inducing the expression of Slug, which represses E-cadherin transcription. E-cadherin inhibits the formation of the β-catenin:TCF complex by sequestering β-catenin in the adhesion pool. β-catenin can relocate back to the cytosol and be degraded after dissociation from E-cadherin or endocytosis of the E-cadherin:β-catenin complex. The premise that β-catenin can be removed by degradation from the adhesion pool, but not from the signaling pool establishes a continuous flux of β-catenin from the signaling to the adhesion pool, which counterbalances the Wnt induced formation of the β-catenin:TCF complex. Thus, our model provides an explanation for the experimental observation that E-cadherin can downregulate the signaling function of β-catenin even when a Wnt stimulus is present (Herzig et al., 2007).

In order to investigate how cytosolic β-catenin distributes into its different protein interaction complexes, we simulated the dynamics of β-catenin containing protein complexes over a timecourse of 8 hours under unperturbed conditions, i.e. in the absence of Wnt signals and APC mutations (Figure 2C). Initially, free cytosolic β-catenin rapidly bound to TCF and APC at the early timepoints. However, over time most of β-catenin became sequestered by E-cadherin, and after 8 hours >90% of β-catenin had migrated into the E-cadherin complex. This result is consistent with the constitutive flux of β-catenin from the cytosol to the membrane predicted by our model and also with experimental observations that in normal cells β-catenin is mainly found in complex with E-cadherin ensuring proper cell adhesion (Lecuit and Lenne, 2007; Nagafuchi and Takeichi, 1988; Wijnhoven et al., 2000). Our simulation predicts that after Wnt-stimulation newly synthesized β-catenin first enters the signaling pool and then is re-distributed to the

adhesion pool. The reason for this dynamic behavior does not lie in the parameter set for the reactions, but is mainly determined by the model structure. For example, newly synthesized β-catenin requires reactions 8, 10, 11 and 16 to form an adhesion complex, while it requires only reaction 9 to form a signaling complex. Therefore, the signaling pool takes up β-catenin faster, but has a lower capacity for β-catenin than the adhesion pool, with the consequence that β-catenin first accumulates in the signaling pool but then re-distributes into the adhesion pool over time. Having established that under unperturbed conditions the E-cadherin adhesion complex is the prevalent destination for β-catenin, we next analyzed the role of APC functionality. APC constrains Wnt signaling by competing with TCF for binding to β-catenin, whereas it positively regulates cellular adhesion by binding and delivering β-catenin to adhesion complexes in the membrane. The vast majority of APC mutations in CRC are truncations that compromise the ability of APC to bind β-catenin (Leedham et al., 2012; van Leeuwen et al., 2007). Thus, changes in APC functionality can be modeled as changes in the levels of wildtype APC. Therefore, we tested the effects of different levels of APC expression and Wnt signaling on the formation of the β-catenin:TCF complex (Figure 2D) and E-cadherin expression (Figure 2E). For each different expression level of APC, low (4ng/ml) and high (400ng/ml) levels of Wnt stimulus were applied. Under these conditions the response profile of E-cadherin expression could be divided into two different zones. In zone 1 Wnt stimulation played an inhibitory role, whereas in zone 2 it enhanced the expression of E-cadherin. Decreasing APC function from high to low levels induced a monotonic increase of the β-catenin:TCF complex (Figure 2D). At low Wnt stimulation this increase occurred at low APC levels. High Wnt stimulation increased the concentration of the β-catenin:TCF complex at high APC levels and reached saturation at intermediate APC levels. On the other hand, E-cadherin expression was high when APC function

was high, and fell as APC levels declined (Figure 2E). Interestingly, while Wnt stimulation increased the abundance of the β-catenin:TCF complex at all APC levels, it increased E-cadherin expression only at high APC levels, but suppressed it when APC levels were low. Thus, the inhibitory effects of Wnt signaling on E-cadherin expression are most severe when APC function is already low. The phase plane analysis integrates the results of Figure 2D and E, and shows the ratio of β-catenin within signaling complex to that within adhesion complex is controlled by APC expression levels (Figure 2F).

These patterns result from APC controlling the balance of β-catenin distribution between the signaling and adhesion pools (Figure 2G-J). A decrease in APC increases the efficiency of assembling β-catenin into signaling complex with TCF, whereas it reduces APC shuttling. Consequently, Wnt signaling is enhanced resulting in the induction of Slug and subsequent repression of E-cadherin expression (Figure 2H). In the absence of Wnt stimulation this balance is stable over a wide range of intermediate APC concentrations. This prediction is consistent with experimental data obtained from cell lines with functional APC and E-cadherin expression (Hendriksen et al., 2008; Yokoyama et al., 2007). However, as Wnt stimulation increases, the balance breaks down to favor adhesion when APC is high (Figures 2I,J), and TCF signaling when APC expression is low. Such a role change results from the competition between the signaling and adhesion pools for β-catenin.

Wnt stimulation increases the β-catenin:TCF complex (i.e. the Wnt signaling complex) at all levels of APC resulting in enhanced Slug expression and suppression of E-cadherin transcription. Thus, the stimulatory effect of Wnt signaling on adhesion complex formation cannot arise from a decreased transcriptional repression of E-cadherin. Rather, this observation arises from the effect that the basal level degradation rate of E-cadherin is higher than that of ubiquitinated E-cadherin

(or of complexed E-cadherin), so that its binding to β-catenin protects E-cadherin from degradation. This prediction is in full agreement with experimental data (Huber et al., 2001). Therefore, the protective effect of β-catenin binding overcomes transcriptional inhibition of E-cadherin expression by Slug, resulting in the increase of E-cadherin levels.

**E-cadherin and APC shuttling cooperate to inhibit Wnt signaling**

We investigated the relative amount of β-catenin assembled in signaling β-catenin:TCF ($S_S$), adhesion ($S_A$), and APC shuttling ($S_T$) complexes. To visualize the three state trajectories at the same time on two-dimensional space, we employed a ternary plot where a point represents the relative ratio of ternary states at each time point. We first investigated the relaxation dynamics of this system for the same initial unstimulated condition as in Figure 2C. For this condition the ternary state trajectory rotated clockwise, which means that a large portion of β-catenin flows from the signaling pool into the APC shuttling pool and from there into the adhesion pool (Figure S1A). At steady state, more than 90% of β-catenin is predicted to be in the adhesion pool. This result is consistent with the experimental observation that in normal crypt cells β-catenin is mainly found in the membrane compartment (Anderson et al., 2002).

Next, we perturbed the steady state with a half-maximal Wnt stimulus and monitored the ternary state change of β-catenin distribution. In the wildtype condition, Wnt did not significantly alter the steady state distribution only slightly shifting it up towards the shuttling pool (Figure S1B). This implies that under normal conditions the increase in β-catenin levels induced by Wnt is absorbed by APC into the shuttling pool rather than by TCF into the signaling pool.

APC and E-cadherin are important mutational targets in CRC and hereditary diffuse gastric cancer (Corso et al., 2012), respectively. To investigate the effect of such mutations, we carried

out simulations where the functionalities of APC and E-cadherin were reduced by decreasing APC abundance and the E-cadherin synthesis rate $A_E$, respectively. When E-cadherin was reduced, the ternary state shifted strongly towards the shuttling pool (APC), meaning that surplus β-catenin was mostly absorbed by APC (Figure S1B). As a result, the signaling pool remained at a similar low level as under wildtype conditions. However, when APC functionality was decreased, Wnt stimulation drove the ternary state from the adhesion pool to the signaling pool (Figure S1B). Ternary plot analysis showed that the relative distribution of β-catenin between the signaling and adhesion pools is robust to Wnt stimulus (Figure S1B). The degradation step of β-catenin after its internalization from the adhesion pool causes a continuous flux of β-catenin from the signaling pool to the adhesion pool. Here, APC shuttling plays a critical role in causing the flux. We further confirmed this with local sensitivity analysis where the output is set to the relative distribution of β-catenin between signaling and adhesion pools. As a result, we found that the relative distribution is only sensitive to the following parameters, $k_{8f/r}$ (APC-β-catenin binding), $k_{9f/r}$ (TCF-β-catenin binding), $k_{10}$ (APC shuttling), $k_{18}$ (internalization of ubiquitinated adhesion complex) (Figure S2B). These parameters are related to the regulation of β-catenin flux to the membrane, and, therefore, are important to establish the relative distribution of β-catenin. This result indicates that Wnt signaling is inhibited by E-cadherin in cooperation with APC shuttling, and that reduction of APC function increases Wnt sensitivity in terms of transcriptional activation. In accordance with Figure S1B, the distribution ratio of β-catenin with respect to its binding partners is abruptly changed when APC functionality is decreased to 3% (the 3rd column in Figure S1C). Interestingly, the total amount of β-catenin is decreased by APC knockdown. This means that APC plays an important role in maintaining the total amount of β-catenin.

**APC plays a crucial role in establishing an adhesion gradient along the crypt**

We further extended our analysis of cellular dynamics to the level of simulating cell migration within a crypt. As described above, the profiles of Wnt signaling, as well as expression of Wnt, E-cadherin, and APC change along the crypt axis. For instance, Wnt signaling decreases upwards the crypt axis (Fevr et al., 2007), whereas APC and E-cadherin expression increases (Escaffit et al., 2005; Senda et al., 2007) (Figure 1D). Total β-catenin seems to be constant (or slightly increasing) along the crypt axis (Aust et al., 2001; Escaffit et al., 2005; Iwamoto et al., 2000). Regression analysis showed that β-catenin expression actually increases along the crypt (Figure S3C). Crypt cells are replenished from the stem cells dividing at the bottom of crypt, and then migrate up towards the top of the crypt, where they are shed into the gut lumen. Thus, every 'individually migrating cell (IMC)' changes its characteristic signaling and expression profiles as it moves upwards along the crypt axis (Figure 3A). In addition, we assumed that the subcellular interaction network comprising β-catenin, TCF, APC, and E-cadherin is at its quasi steady state at each IMC position in the crypt, since the dynamics of this subcellular network is much faster than cell migration speed. Based on these premises we constructed a mathematical model of the IMC by imposing the changing extracellular Wnt ligand and the subcellular APC expression profiles on the subcellular interaction network. The Wnt stimulation profile decreases (Medema and Vermeulen, 2011), while APC expression increases from bottom to top of the crypt (Aust et al., 2001; Fodde et al., 2001; Gaspar and Fodde, 2004; Long et al., 2011; Midgley et al., 1997; Senda et al., 2007; Smith et al., 1993). Since the experimental data regarding APC expression along crypt tissue in mammalian and Wingless (Wnt) profile in *Drosophila* wing development showed exponential changes, we employed an exponential function to model the profiles of APC expression and Wnt ligands along the crypt (Supplemental Materials and Methods) (Kicheva et

al., 2007; Senda et al., 2007). Thus, the distribution of Wnt ligand along the crypt axis was modeled as

$$W(x) = W_{Max} \exp(-x / \alpha_{Wnt})$$

where $x$ indicates the normalized position along the crypt axis between 0 (bottom) and 1 (top of the crypt), $W_{Max}$ denotes the maximum Wnt stimulus, and $\alpha_{Wnt}$ indicates the decay coefficient. The expression of APC along the crypt axis was modeled as

$$APC_{Total}(x) = \frac{A}{\exp(\alpha_{APC}{}^{-1})}\left[\exp(\alpha_{APC}{}^{-1}x) - 1.0\right] + APC_{Min}$$

where $APC_{Min}$ indicates the total APC within a cell at the bottom of crypt, and $A$ and $\alpha_{APC}$ denote the coefficients of an exponential function.

We first confirmed that the IMC model could reproduce the changes in Wnt signaling (as measured by formation of the β-catenin:TCF complex), E-cadherin and β-catenin expression profiles along the crypt that are consistent with experimental observations. Randomly generated coefficients (population size: 1000) for the profiles of APC expression and Wnt ligands were used to simulate the IMC model. We found that more than 85% of the population are concordant with the experimental molecular profiles of β-catenin, E-cadherin, and Wnt activity (Figures 3H,I and Figures S3B,C) (Fevr et al., 2007). This means that the model not only well explains the experimental observations, but also that the model is not sensitive to variations in parameter values.

Interestingly, for all sets of the coefficients that are concordant with the experimental pattern of profiles (β-catenin, E-cadherin, and Wnt activity), the IMC model predicted that the adhesion profile (as measured by the formation of the adhesion pool) increased along the crypt axis, while

the β-catenin signaling pool decreased (first row of Figure 4B and Figures 3G,J). This shift is due to the APC gradient increasing towards the top of the crypt causing a migration of β-catenin from the signaling pool to the adhesion pool (Figures 2F, 2I, and 3B). This result is supported by experimental observations, where reconstitution of wildtype APC expression in mutant APC cells enhanced cell adhesion (Faux et al., 2004), whereas truncation of one APC allele in $APC^{Min/+}$ mice decreased the formation of adhesion complexes (Carothers et al., 2001). The increasing expression of APC towards the top of the crypt is essential for the formation of the increasing E-cadherin-mediated adhesion gradient. Since free E-cadherin without its binding partner (β-catenin) does not have the adhesion function (Lecuit and Lenne, 2007; Nagafuchi and Takeichi, 1988), we only considered the adhesion complex (β-catenin:E-cadherin) to measure the adhesion level of a cell and assumed that adhesion is linearly proportional to the number of adhesion complexes in membrane compartment.

Our results imply that the increasing profile of APC plays an essential role in establishing the molecular profiles (β-catenin, E-cadherin, and Wnt activity) because APC controls the distribution ratio of β-catenin with respect to its binding partners, TCF and E-cadherin (Figures 2F, 3B). To confirm such essentiality of APC gradient, we modeled the IMC in a crypt without APC gradient using a constant APC profile along the crypt (Figure S3D). Five different crypts of five constant concentrations (0.1, 1, 10, 100, and 200 nM) of APC expression were considered to simulate the IMC model. We found that for all the constant profiles of APC the signaling β-catenin complex decreased towards the top of the crypt similar as in a normal crypt, which is in contrast to experimental data showing that β-catenin and E-cadherin increase towards to top of the crypt (Figure S3D). Therefore, we conclude that wildtype APC expression coordinates the proper formation of β-catenin signaling and adhesion pools, thereby establishing an adhesion

gradient along the crypt. We used a genetic algorithm to establish a reference coefficient set that fits the experimental data for APC expression and Wnt ligand profile along the crypt (Supplemental Materials and Methods).

**Spatial signaling and adhesion gradients in the crypt facilitate the elimination of mutated cells with a high proliferative potential**

The simulation results shown in Figure 4 are schematically summarized in Figure S4C-E showing that a mutated cell re-positions itself in the crypt epithelium driven by the adhesion gradient (Figure S4C) and will migrate either towards the top or bottom of the crypt depending on the direction of the adhesion gradient (Figures S4D,E). These simulations predict that crypts that retain 50% APC function, as would be the case in heterozygous mutations, still can efficiently eliminate mutated cells (i.e. cells with Wnt signaling mutations resulting in the increase of proliferation rate). In contrast, if APC function is severely reduced, mutated cells (with somatic mutation) are retained in the crypt and can initiate the conversion of benign hyperplasia and adenoma to malignant carcinomas. These theoretical predictions are consistent with experimental observations that the Wnt pathway is activated in two steps during colorectal carcinogenesis (Najdi et al., 2011). The first step is APC mutation, which causes benign adenomas, while the second step causes additional stimulation of Wnt signaling and tumor progression. This second step usually increases the transcriptional activity of the Wnt pathway, which induces the expression of proliferation promoting genes, and can be caused by various mechanisms including the autocrine production of Wnt ligands (Park et al., 2009; Smith et al., 1999), the silencing of Wnt pathway repressors (Aguilera et al., 2006; Caldwell et al., 2004; González-Sancho et al., 2005; Suzuki et al., 2004), the promotion of β-catenin accumulation in the nucleus caused by Rac activation (Wu et al., 2008) or KRAS mutations (Phelps et al., 2009).

According to our model such cells with increases in Wnt signaling still should be eliminated as long as enough APC function is available to maintain the adhesion gradient that drives cell migration up the crypt. However, once this gradient is subverted mutated cells are retained and tumor progression can ensue. Thus, APC function is a critical gatekeeper in the pathogenesis of CRC.

## SUPPLEMENTAL DISCUSSION

Interestingly, c-Myc gene deletion largely restores intestinal homeostasis and architecture in $APC^{-/-}$ mice (Sansom et al., 2007). It seems not clear how c-Myc fits into the role of APC in the elimination of hyper-proliferating cells based on adhesion as outlined in the model. Actually, the rescue of APC deficiency by deletion of c-Myc can be explained by the model. The deletion of c-Myc increases E-cadherin expression because c-Myc suppresses E-cadherin (Ma et al., 2010), and the increased E-cadherin functionality (forming adhesion complex by binding β-catenin) compensates for the weakened APC shuttling caused by APC deficiency. The increase of E-cadherin expression decreases cell proliferation by suppressing the transcriptional activity of β-catenin (Nelson and Nusse, 2004). Therefore, the deletion of c-Myc not only recovers the adhesion function of E-cadherin but also decreases the proliferation of APC mutated cells. These observations explain how the deletion of c-Myc could dampen APC mutant phenotypes. This is actually another good example supporting the explanatory power of our model.

## SUPPLEMENTAL MATERIALS AND METHODS

**Model assumptions.**

Model assumptions are mostly explained in the Supplemental Results. Since the directed motion of the KIF3A-KIF3B kinesin complex along microtubules drives the active transport of APC and APC:β-catenin complex towards membrane, we assumed that such active transports can be represented by the following unidirectional reactions:

$$[\mathrm{APC}] \xrightarrow{k_{12f}} [\mathrm{APC_M}]$$

$$[\mathrm{APC{:}\beta\text{-}catenin}] \xrightarrow{k_{10}} [\mathrm{APC_M{:}\beta\text{-}catenin_M}]$$

where the suffix M indicates the membrane localization of the molecular components.

**Parameter optimization and screening.**

Parameter estimation was done using genetic algorithms (GA). The built-in GA of Matlab (Version 7) was employed to find the optimal parameter set that fits experimental data (http://www.mathworks.co.kr/discovery/genetic-algorithm.html). The fitness function of GA is defined by

$$f = \frac{1}{N}\sum_{i}^{N}\left(C_i - C_i'\right)^2$$

where $C_i$, $C_i'$, and $N$ denote the experimental data point, the predicted data point, and the number of data points, respectively. The detailed steps of parameter optimization and screening can be found in Parameter Estimation, Table S1, and Table S2.

**Bifurcation analysis.**

To investigate the change of steady state of signaling complex (β-catenin:TCF) and adhesion

complex (β-catenin:E-cadherin) when the E-cadherin expression rate varies, we employed the numerical continuation method using AUTO07p (http://cmvl.cs.concordia.ca/auto/).

**Ternary plot analysis.**

The subcellular molecular interaction network consists of two direct competitions of TCF vs. APC in the cytoplasm and APC vs. E-cadherin at the cell membrane, and one indirect competition of TCF vs. E-cadherin. To examine the dynamic redistribution of β-catenin into its binding partners driven by the competitions, we employed a graphical analysis method based on ternary plots to investigate the molecular distribution at steady state. A ternary plot is a barycentric plot which graphically depicts the ratios of three variables as positions in an equilateral triangle. The proportions of the three variables a, b, and c must sum to a constant, K, usually represented as 1 or 100%. Since the amount of the destruction complex is relatively very small, we assumed that the total amount of β-catenin is $Cat_{Total} = Cat_{APC} + Cat_{TCF} + Cat_{Cadherin}$ (Lee et al., 2003; Tan et al., 2012). So, $Cat_{APC}$, $Cat_{TCF}$, and $Cat_{Cadherin}$ are the three components that constitute our ternary graph. Each component is divided by the total sum of all components for normalization into a ratio as $\overline{S}_k = \frac{S_k}{\sum_{k=1}^{3} S_k}$. Each component represents the ratio of β-catenin bound to TCF, E-cadherin, or APC, which are designated as Signaling (S), Adhesion (A) and Shuttling (T) pools, respectively. Here, each component is defined as follows: $S_S$ = [βCat:TCF], $S_A$ = [ECAD: $\beta Cat_M$] + [$ECAD^{UB}$: $\beta Cat_M{}^{UB}$] + [$ECAD_I{}^{UB}$:$\beta Cat_I{}^{UB}$], and $S_T$ = [βCat:APC] + [$\beta Cat_M$:$APC_M$] where [ECAD: $\beta Cat_M$], [$ECAD^{UB}$: $\beta Cat_M{}^{UB}$], and [$ECAD_I{}^{UB}$:$\beta Cat_I{}^{UB}$] indicate adhesion complex, ubiquitinated adhesion complex, and ubiquitinated internalized adhesion complex, respectively.

**A force model based on the differential adhesion.**

In particular, we investigated the effect of somatic mutations that enhance Wnt signaling and result in cells with a higher proliferative potential than normal neighboring cells. Such mutations can also change the amount of adhesion complexes within a cell, and subsequently induce a different adhesion level between the mutated cell and its normal neighboring cells. It is obvious that increased proliferation will give selective advantage to the mutated cell in the crypt environment. By contrast, the effect of the different adhesion level is not clear. To investigate the effect of this 'adhesion difference', we employed the differential adhesion model which posits that cells rearrange their positions to minimize the total sum of their adhesion differences. This model has been experimentally verified in a number of biological species driving the re-positioning and migration of cells during tissue and organ formation in development (Foty and Steinberg, 2005; Hammerschmidt and Wedlich, 2008; Lecuit and Lenne, 2007; Steinberg, 2007). For instance, during development of the zebrafish gastrula an adhesion gradient guides unidirectional cell migration, where cells move towards higher adhesion (Hardt et al., 2007). Based on these observations, we assumed that there exists a rearranging force proportional to the adhesion gradient and the adhesion difference. We modeled the force, which a mutated cell would experience depending on its position in the crypt and the differences in adhesion as follows:

$$F(x) = \gamma A_0'(x)\left[A_1(x) - A_0(x)\right]$$

where $A_1(x)$, $A_0(x)$, $A_0'(x)$, and $\gamma$ are the altered adhesion level by mutation, the normal adhesion level, the adhesion gradient at a crypt position $x$, and a proportionality constant,

respectively. Positive force $F(x)>0$ means that the mutated cell moves towards the top of the crypt ($x=1$). Hence, if the gradient of adhesion is positive $A_0'(x) = dA_0(x)/dx > 0$ and a mutated cell has a positive difference of adhesion, the mutated cell moves towards the top of the crypt (Figure 3C). In case of a normal cell, the induced force, $F(x)$ is zero because $A_1=A_0=0$. This, however, does not mean that normal crypt cells do not migrate. Normal crypt cells can still migrate by other migration mechanisms such as migration by mitotic pressure and active cell migration (Heath, 1996). Zero force $F(x)=0$ means that there is no directed force induced from the difference in adhesion. Negative force $F(x)<0$ means that the mutated cell moves towards the bottom of the crypt ($x=0$).

**A model for β-catenin exon 3 mutation.**

The most common mutations in β-catenin gene in cause colon cancer target exon 3 (Morin et al., 1997), where the phosphorylation by GSK3β occurs. Thus, exon 3 mutations can lead to constitutive activation of β-catenin without APC mutation (Iwao et al., 1998; Zhu et al., 2009). Exon 3 mutations are also known to reduce the localization of β-catenin to the cell membrane and thereby alter the formation of adhesion complexes (Han et al., 2013; Kawanishi et al., 1995). Structural studies have shown that β-catenin has a single shared interaction domain, consisting of 12 armadillo repeats, where the binding sequences of its interaction partners significantly overlap with each other (Bienz and Clevers, 2003; Hülsken et al., 1994; von Kries et al., 2000). This means that β-catenin mutation might equally affect the kinetic parameters for β-catenin phosphorylation and E-cadherin binding. Based on these experimental observations we mimicked exon 3 mutation of β-catenin by decreasing the kinetic parameters for the phosphorylation of β-catenin ($k_6$) and E-cadherin binding ($k_{16f}$) by 2% (compared to wildtype) in

our mathematical model.

# Experimental evidence used for constructing the mathematical model

### Wnt signaling pathway module

The central role of Wnt signaling pathway is to regulate the destruction machinery of β-catenin (MacDonald et al., 2009). Extracellular Wnt stimulates inactivation of the destruction complex (DC) that consists of APC, Axin, CK1, and GSK3β. Consequently, β-catenin accumulates in the cytoplasm. Accumulated β-catenin assembles into signaling complex with TCF, leading to transcription of Wnt target genes. In the absence of Wnt stimulus, DC phosphorylates the amino terminal region of β-catenin, resulting in β-catenin recognition by β-TrCP, an E3 ubiquitin ligase subunit, and subsequent proteasomal degradation. We adapted the previous model by Lee et al. to build a Wnt pathway module that is represented by reactions 1-9, 24, and 26 in Figure 1B (Lee et al., 2003).

### Crosstalk effect of Wnt signaling and adhesion

The transcriptional cofactor β-catenin also plays a role in cellular adhesion by binding to E-cadherin in the membrane (Nelson and Nusse, 2004; Stepniak et al., 2009). Although its signaling partner (TCF) and adhesion partner (E-cadherin) are localized to different cellular compartments (cytoplasm and membrane, respectively), there are crosstalk effects between the signaling and adhesion pools (Jeanes et al., 2008).

Bienz et al. suggested an APC-shuttling based mechanism to explain the functional crosstalk effects (Bienz, 1999). According to this mechanism, APC picks up β-catenin in the cytoplasm or nucleus, and then delivers it to the membrane by an unknown transport mechanism. The β-catenin delivered to the cell membrane then can associate with E-cadherin to assemble an adhesion complex. This suggestion is supported by many experimental observations. APC moves along microtubule structures (Hirokawa and Noda, 2008; Mimori-Kiyosue et al., 2000). Hence, the experimental evidence of β-catenin co-precipitation with the kinesin containing APC-KAP3-KIF3A-KIF3B complex (Jimbo et al., 2002) suggested that APC and β-catenin are transported towards the membrane along microtubules by the KAP3-KIF3A-KIF3B complex. Moreover, Klingelhöfer et al. observed that free cytoplasmic β-catenin exchanged with E-cadherin-bound β-catenin in pulse labeling experiments (Klingelhöfer et al., 2003). Such an effect was significantly repressed in APC mutated cells. Based on these observations, we assumed that the APC shuttling processes as follows: (1) Both APC and APC:β-catenin in the cytoplasm actively translocate to the membrane with the help of kinesin motor proteins using the chemical energy of ATP. (2) The APC:β-catenin at the membrane is disassembled into free APC and free β-catenin. (3) One part of free APC at the membrane competes with free E-cadherin to bind with free β-catenin, and the other part of free APC at the membrane dissociates to the cytoplasm. (4) Free β-catenin located at the membrane partly dissociates to the cytoplasm. (5) At the membrane, free E-cadherin interacts with free β-catenin delivered by APC. This shuttling process is represented by the reactions 10, 11, $12_r$, $12_f$, 16, and 23 in Figure 1B.

**Adhesion junction remodeling pathway**

Although both E-cadherin and E-cadherin:β-catenin exist in the membrane, only the adhesion complex E-cadherin:β-catenin can promote cellular adhesion. Interestingly, static cellular contact

established by adhesion junction is regulated by the dynamic process in which adhesion complexes are internalized, ubiquitinated, and partially recycled (De Beco et al., 2009; Fujita et al., 2002; Harris and Tepass, 2010; Ishiyama et al., 2010; Le et al., 1999; Pece and Gutkind, 2002). Moreover, Le et al. suggested that a pool of surface E-cadherin is constantly remodeled via endocytic recycling process in their cell culture experiments (Le et al., 1999). We included this process to construct a more general model that represents crypt epithelial cells. The adhesion junction remodeling can be characterized by the following three processes (Fujita et al., 2002; Pece and Gutkind, 2002). First, ubiquitin chains are transferred to both E-cadherin and β-catenin through the E1/E2/E3 ubiquitination system. Second, ubiquitinated β-catenin is degraded in the proteasome. Third, E-cadherin is degraded in the proteasome or partially recycled. The adhesion junction remodeling is represented by the reactions 17-22, and 25 in Figure 1B.

**Transcriptional repression of E-cadherin by β-catenin's signaling function**

β-catenin's signaling function transcriptionally inhibits E-cadherin *in vivo* and *in vitro*. Such inhibition is regulated directly or via an E-cadherin inhibitor, Slug (Conacci-Sorrell et al., 2003; Jamora et al., 2003). These processes are represented by the gene regulatory processes 13, 14, and 15 in Figure 1B.

# Mathematical model

**The detailed biochemical reactions of the Wnt signaling pathway and the E-cadherin-mediated adhesion system**

| Reaction | Description |
|---|---|
| $[DC] \xrightarrow{r_1} [APC:Axin] + [GSK3\beta]$ | Dissociation reaction of APC-Axin complex and GSK3β controlled by extracellular Wnt stimulus |
| $[APC:Axin] + [GSK3\beta] \xleftrightarrow{r_2} [DC]$ | Association and dissociation reaction of APC-Axin complex and GSK3β |
| $[\beta Cat] \xrightarrow{r_3} \phi$ | Degradation reaction of β-catenin |
| $\phi \xrightarrow{r_4} [\beta Cat]$ | De novo synthesis reaction of β-catenin |
| $[DC] + [\beta Cat] \xleftrightarrow{r_5} [DC:\beta Cat]$ | Association and dissociation reaction of DC and β-catenin |
| $[DC:\beta Cat] \xrightarrow{r_6} [DC:\beta Cat^P]$ | Phosphorylation reaction of β-catenin by DC |
| $[DC:\beta Cat^P] \xrightarrow{r_7} [DC] + [\beta Cat^P]$ | Dissociation reaction of DC and (phosphorylated) β-catenin complex |
| $[APC] + [\beta Cat] \xleftrightarrow{r_8} [APC:\beta Cat]$ | Association and dissociation reaction of APC and β-catenin |
| $[\beta Cat] + [TCF] \xleftrightarrow{r_9} [TCF:\beta Cat]$ | Association and dissociation reaction of TCF and β-catenin |
| $[APC:\beta Cat] \xrightarrow{r_{10}} [APC_M:\beta Cat_M]$ | Active transporting of cytoplasmic APC-β-catenin complex towards membrane |
| $[APC_M] + [\beta Cat_M] \xleftrightarrow{r_{11}} [APC_M:\beta Cat_M]$ | Association and dissociation reaction of APC and β-catenin in membrane |
| $[APC] \xrightarrow{r_{12f}} [APC_M]$ | Active transporting of cytoplasmic APC towards membrane |
| $[APC_M] \xrightarrow{r_{12r}} [APC]$ | Dissociation reaction of membrane APC into cytoplasm |
| $Gene \xrightarrow{r_{13}} [Snail]$ | Gene regulation. Transcriptional activation of β-catenin-TCF complex expresses Snail in nucleus |
| $Gene \xrightarrow{r_{14}} [ECAD]$ | Gene regulation. Snail transcriptionally inhibits the expression of E-cadherin in nucleus |
| $Gene \xrightarrow{r_{15}} [ECAD]$ | Gene regulation. β-catenin-TCF complex transcriptionally inhibits the expression of E-cadherin in nucleus |
| $[ECAD] + [\beta Cat_M] \xleftrightarrow{r_{16}} [ECAD:\beta Cat_M]$ | Association and dissociation reaction of E-cadherin and β-catenin in membrane |
| $[ECAD:\beta Cat_M] \xrightarrow{r_{17}} [ECAD^{UB}:\beta Cat_M{}^{UB}]$ | Ubiquitination of adhesion complex (E-cadherin:β-catenin) in membrane |
| $[ECAD^{UB}:\beta Cat_M{}^{UB}] \xrightarrow{r_{18}} [ECAD_I{}^{UB}:\beta Cat_I{}^{UB}]$ | Internalization of ubiquitinated adhesion complex (E-cadherin:β-catenin) in membrane |

| | |
|---|---|
| $\left[ECAD_I^{UB} : \beta Cat_I^{UB}\right] \xrightarrow{r_{19}} \left[ECAD_I^{UB}\right] + \left[\beta Cat_I^{UB}\right]$ | Dissociation reaction of ubiquitinated adhesion complex (E-cadherin:β-catenin) in cytoplasm |
| $\left[\beta Cat_I^{UB}\right] \xrightarrow{r_{20}} \phi$ | Degradation reaction of ubiquitinated β-catenin in cytoplasm |
| $\left[ECAD_I^{UB}\right] \xrightarrow{r_{21}} \left[ECAD_I\right]$ | De-ubiquitination of ubiquitinated E-cadherin in cytoplasm |
| $\left[ECAD_I^{UB}\right] \xrightarrow{r_{22}} \phi$ | Degradation reaction of ubiquitinated E-cadherin in cytoplasm |
| $\left[\beta Cat_M\right] \xrightarrow{r_{23}} \left[\beta Cat\right]$ | Dissociation reaction of membrane β-catenin into cytoplasm |
| $\left[\beta Cat^P\right] \xrightarrow{r_{24}} \phi$ | Degradation reaction of phosphorylated β-catenin in cytoplasm |
| $\left[ECAD_I\right] \xrightarrow{r_{25}} \left[ECAD\right]$ | Exocytosis of internalized E-cadherin towards membrane |
| $\left[APC\right] + \left[Axin\right] \xleftrightarrow{r_{26}} \left[APC : Axin\right]$ | Association and dissociation reaction of APC and Axin |
| $\left[ECAD\right] \xrightarrow{r_{27}} \phi$ | Degradation reaction of E-cadherin |

**The mathematical model of the Wnt signaling pathway and the E-cadherin-mediated adhesion system**

$$\frac{d\left[DC\right]}{dt} = -k_{5f}\left[DC\right]\left[\beta Cat\right] - \omega\left[DC\right] + k_{5r}\left[DC : \beta Cat\right] - k_{2r}\left[DC\right] + k_7\left[DC : \beta Cat^P\right] + k_{2f}\left[APC : Axin\right]$$

$$\frac{d\left[APC : Axin\right]}{dt} = \omega\left[DC\right] - k_2\left[APC : Axin\right]\left[GSK3\beta\right] - k_{26r}\left[APC : Axin\right] + k_{26f}\left[APC\right]\left[Axin\right]$$

$$\frac{d\left[\beta Cat\right]}{dt} = k_4 - k_{5f}\left[DC\right]\left[\beta Cat\right] + k_{5r}\left[DC : \beta Cat\right] - k_{9f}\left[TCF\right]\left[\beta Cat\right] + k_{9r}\left[TCF : \beta Cat\right] - k_3\left[\beta Cat\right] + k_{8r}\left[APC : \beta Cat\right] + k_{23}\left[\beta Cat_M\right] - k_{8f}\left[\beta Cat\right]\left[APC\right]$$

$$\frac{d\left[DC : \beta Cat\right]}{dt} = -k_6\left[DC : \beta Cat\right] + k_{5f}\left[DC\right]\left[\beta Cat\right] - k_{5r}\left[DC : \beta Cat\right]$$

$$\frac{d\left[DC : \beta Cat^P\right]}{dt} = k_6\left[DC : \beta Cat\right] - k_7\left[DC : \beta Cat^P\right]$$

$$\frac{d\left[\beta Cat^{P}\right]}{dt} = -k_{24}\left[\beta Cat^{P}\right] + k_{7}\left[DC:\beta Cat^{P}\right]$$

$$\frac{d\left[APC\right]}{dt} = \begin{array}{c} -k_{12f}\left[APC\right] + k_{8r}\left[APC:\beta Cat\right] + k_{12r}\left[APC_{M}\right] - k_{8f}\left[\beta Cat\right]\left[APC\right] \\ -k_{26f}\left[Axin\right]\left[APC\right] + k_{26r}\left[APC:Axin\right] \end{array}$$

$$\frac{d\left[APC:\beta Cat\right]}{dt} = -k_{10}\left[APC:\beta Cat\right] - k_{8r}\left[APC:\beta Cat\right] + k_{8f}\left[\beta Cat\right]\left[APC\right]$$

$$\frac{d\left[TCF\right]}{dt} = -k_{9f}\left[TCF\right]\left[\beta Cat\right] + k_{9r}\left[TCF:\beta Cat\right]$$

$$\frac{d\left[TCF:\beta Cat\right]}{dt} = k_{9f}\left[TCF\right]\left[\beta Cat\right] - k_{9r}\left[TCF:\beta Cat\right]$$

$$\frac{d\left[APC:\beta Cat_{M}\right]}{dt} = k_{10}\left[APC:\beta Cat\right] + k_{11f}\left[\beta Cat_{M}\right]\left[APC_{M}\right] - k_{11r}\left[APC:\beta Cat_{M}\right]$$

$$\frac{d\left[APC_{M}\right]}{dt} = -k_{11f}\left[\beta Cat_{M}\right]\left[APC_{M}\right] + k_{12f}\left[APC\right] - k_{12r}\left[APC_{M}\right] + k_{11r}\left[APC_{M}:\beta Cat_{M}\right]$$

$$\frac{d\left[\beta Cat_{M}\right]}{dt} = \begin{array}{c} -k_{16f}\left[ECAD\right]\left[\beta Cat_{M}\right] - k_{11f}\left[\beta Cat_{M}\right]\left[APC_{M}\right] + k_{16r}\left[AC\right] - k_{23}\left[\beta Cat_{M}\right] \\ +k_{11r}\left[APC_{M}:\beta Cat_{M}\right] \end{array}$$

$$\frac{d\left[ECAD\right]}{dt} = -k_{16f}\left[ECAD\right]\left[\beta Cat_{M}\right] - k_{27}\left[ECAD\right] + k_{16r}\left[AC\right] + k_{21}\left[ECAD^{UB}\right] + \chi$$

$$\frac{d\left[AC\right]}{dt} = k_{16f}\left[ECAD\right]\left[\beta Cat_{M}\right] - k_{16r}\left[AC\right] - k_{17}\left[AC\right]$$

$$\frac{d\left[ECAD^{UB}\beta Cat^{UB}\right]}{dt} = -k_{18}\left[ECAD^{UB}\beta Cat^{UB}\right] + k_{17}\left[AC\right]$$

$$\frac{d\left[ECAD_I^{UB}\beta Cat_I^{UB}\right]}{dt} = -k_{19}\left[ECAD_I^{UB}\beta Cat_I^{UB}\right] + k_{18}\left[ECAD^{UB}\beta Cat^{UB}\right]$$

$$\frac{d\left[ECAD^{UB}\right]}{dt} = k_{19}\left[ECAD_I^{UB}\beta Cat_I^{UB}\right] - k_{22}\left[ECAD^{UB}\right] - k_{21}\left[ECAD^{UB}\right]$$

$$\frac{d\left[\beta Cat^{UB}\right]}{dt} = k_{19}\left[ECAD_I^{UB}\beta Cat_I^{UB}\right] - k_{20}\left[\beta Cat^{UB}\right]$$

$$\frac{d\left[Axin\right]}{dt} = -r_{26f}\left[Axin\right]\left[APC\right] + r_{26r}\left[APC:Axin\right]$$

$$\frac{d\left[GSK3\beta\right]}{dt} = \omega\left[DC\right] - k_2\left[APC:Axin\right]\left[GSK3\beta\right]$$

Mathematical functions are defined as follows:

$$\chi\left(\left[TCF:\beta Cat\right]\right) = \frac{A_E}{1+\left(\left[TCF:\beta Cat\right]/K_{e50}\right)^m}$$

$$\omega\left(\left[Wnt\right]\right) = A_w\left[Wnt\right]$$

where $\omega\left(\left[Wnt\right]\right)$ and $\chi\left(\left[TCF:\beta Cat\right]\right)$ are input functions for Wnt and gene regulation function, respectively. The function $\chi$ is a simplified expression which integrates the reactions 13-15 on Figure 1B, where variable *Slug* is omitted and is not explicitly expressed. The reactions 21 and 25 are integrated by omitting the state variable [$ECAD_I$] to reduce the number

of system equations.

**Description of variables**

| Variable | Description | Variable | Description |
|---|---|---|---|
| $[DC]$ | Destruction complex | $[APC_M : \beta Cat_M]$ | Complex of APC and β-catenin in membrane |
| $[APC : Axin]$ | Complex of APC and Axin | $[APC_M]$ | Free APC in membrane |
| $[\beta Cat]$ | Free β-catenin in cytoplasm | $[\beta Cat_M]$ | Free β-catenin in membrane |
| $[DC : \beta Cat]$ | β-catenin bounded in destruction complex | $[ECAD]$ | Free E-cadherin in membrane |
| $[DC : \beta Cat^P]$ | Phosphorylated β-catenin bounded in destruction complex | $[AC]$ | Adhesion complex (β-catenin:E-cadherin) in membrane |
| $[\beta Cat^P]$ | Phosphorylated β-catenin | $[ECAD^{UB} : \beta Cat^{UB}]$ | Ubiquitinated adhesion complex |
| $[APC]$ | APC in cytoplasm | $[ECAD_I^{UB} : \beta Cat_I^{UB}]$ | Internalized Ubiquitinated adhesion complex |
| $[APC : \beta Cat]$ | Complex of APC and β-catenin in cytoplasm | $[ECAD_I^{UB}]$ | Internalized Ubiquitinated E-cadherin |
| $[TCF]$ | Free TCF | $[\beta Cat_I^{UB}]$ | Internalized Ubiquitinated β-catenin |
| $[TCF : \beta Cat]$ | Transcriptionally active complex of TCF and β-catenin | $[Axin]$ | Free Axin |
| $[GSK3\beta]$ | Free GSK3β | | |

**Total amount of conservative species**

| Species | Description | Numerical value nM | Reference |
|---|---|---|---|
| $APC_0$ | Total amount of *APC* | 35 | (Tan et al., 2012) |
| $Axin_0$ | Total amount of *Axin* | 32 | (Tan et al., 2012) |
| $TCF_0$ | Total amount of *TCF* | 15 | (Tan et al., 2012) |
| $GSK3\beta_0$ | Total amount *GSK3β* | 21 | (Tan et al., 2012) |

**Mass conservation equations**

The total amount of Axin, GSK3β, and TCF are assumed to be constant in this model. For APC, the total amount of APC is assumed to be constant when the simulation is performed at a subcellular level. For the crypt-level simulation, the total amount of APC is changed along the crypt. The mass conservation equations are as follows:

$$TCF_0 = [TCF] + [TCF : \beta Cat]$$

$$APC_0 = \begin{aligned}[t] &[DC : \beta Cat^P] + [DC : \beta Cat] + [DC] + [APC : Axin] + [APC] + [APC : \beta Cat] \\ &+ [APC : \beta Cat_M] + [APC_M] \end{aligned}$$

$$Axin_0 = [Axin] + [APC : Axin] + [DC] + [DC : \beta Cat] + [DC : \beta Cat^P]$$

$$GSK3\beta_0 = [GSK3\beta] + [DC]$$

where $APC_0$, $Axin_0$, $GSK3\beta_0$, and $TCF_0$ are the total amount of each molecular species. The $APC_0$ has the same meaning as $APC_{Total}$ in the main text.

**The mathematical profiles of APC expression and Wnt ligands for the IMC (Individually Migrating Cell) model**

Unlike model systems such as the developing *Drosophila* wing, where Kicheva *et al*. have shown that the Wingless (Wnt) profile decays exponentially (Kicheva et al., 2007), the Wnt profile in intestinal crypts has not been quantitatively measured. From the available qualitative data, where Wnt activity was measured by using conductin-lacZ reporter mice (Fevr et al., 2007), we assumed that the concentration of Wnt ligand along the crypt axis decays exponentially. For APC concentration along the crypt, we quantified the relative APC concentration along the crypt by using the microscopic imaging data reported by Senda et al (Figure S3A). The quantified APC

concentration fits an exponential function (Figure S3A) suggesting that the APC concentration increases exponentially. Therefore, exponential functions are used to model the Wnt and APC profiles where $W_{Max}$ and $\alpha_{Wnt}$ are parameters for the Wnt profile and $A$, $\alpha_{APC}$, and $APC_{Min}$ are parameters for the APC profile, respectively. The formula for $APC_{Total}(x)$ has a more complicated form in order to explicitly parameterize the minimal APC value as $APC_{Min}$.

# Parameter estimation

**Step 1. Parameter estimation using quantitative experimental data for subcellular pathway model.**

Hannoush et al. measured the time-series data of total β-catenin in dependence of stimulating the Wnt pathway in L cells (Hannoush, 2008). It is known that the L cells do not have any E-cadherin. To fit the parameters of our mathematical model to this experimental data, our model system needs to have the same condition as the L cells. This condition can be met by setting $A_E$ (the expression rate of E-cadherin) to zero. With this setting, the mathematical model is reduced to have reactions 1-11, $12_f$, $12_r$, 23, and 26 (Figure 1B). The reduced model is then optimized to fit the time-series data from L cells.

For E-cadherin expressing cells, the number of cellular adhesion molecules (E-cadherin) at the cell surface ranges between $2.37\times10^4$ and $1.58\times10^5$ molecules depending on experimental conditions (Duguay et al., 2003). Since 1 nM is 1000 particles in a single HeLa cell (Moran et al., 2010), we considered that a single cell has 23.7-158 nM of E-cadherin in surface and assumed that epithelial cells have 91 nM (the mean value of the measures) at steady state. Therefore, total surface E-cadherin = $[ECAD] + [AC] = 91$ nM. Moreover, approximately 18% of E-cadherin are

internalized in MDCK cell line (Le et al., 1999). Therefore, internalized E-cadherin is $[ECAD^{UB}{:}\beta Cat^{UB}] + [ECAD_I^{UB}{:}\beta Cat_I^{UB}] + [ECAD^{UB}] = 20$ nM and the total amount of E-cadherin is $[ECAD]+[AC]+[ECAD^{UB}\beta Cat^{UB}]+ [ECAD_I^{UB}{:}\beta Cat_I^{UB}] + [ECAD^{UB}] = 111$ nM. Using these constraints (surface and internalized E-cadherin), we optimized the parameter values for the adhesion remodeling that is represented by reactions 13-22, and 27 in Figure 1B.

Since the parameter set that fits the experimental data regarding β-catenin and E-cadherin is not unique, the optimization process was repeated 1840 times with different initial seeds to obtain a group of parameter sets ($S_1$).

**Step 2. Parameter selection using qualitative experimental data for subcellular pathway model.**

Knocking-down E-cadherin expression in DLD-1 cells, which exhibit E-cadherin-based cell contacts, activated the Wnt signaling pathway suggesting that the normal expression of E-cadherin is sufficient to repress the signaling activity of β-catenin (Kuphal and Behrens, 2006). Most plausibly, such repression of the signaling activity of β-catenin is directly linked to the increase of adhesion because β-catenin signaling is repressed by the binding of E-cadherin to β-catenin at the membrane. Therefore, β-catenin accumulation caused by Wnt stimulation will increase adhesion in normal cells (Bradley et al., 1993; Hinck et al., 1994; Papkoff et al., 1996; Toyofuku et al., 2000). Our model confirmed this hypothesis (Figure 2E,F). In order to assess the influence of parameter variation on the model outcomes we analyzed the effect of E-cadherin expression on the Wnt signaling and the effect of Wnt stimulation on the adhesion complex under different parameter sets (Figure S2A). For this purpose the parameter values were repeatedly estimated to obtain a population of the sets of parameter values (the number of parameter sets, $S_1 = 1840$). As a result, we found that the distribution pattern of the normalized

Wnt response ($R_w$) showed two groups, one at a low (average value: 0.1) and another at a high ratio close to 1 (average value: 0.92) (Figure S2A). The groups of high (sustained) and low (suppressed) Wnt responses were 7% and 93%, respectively. For the high Wnt response region ($R_w > 0.5$), the normalized adhesion change ($R_a$) varied from 0.1 to 10. For the low Wnt signaling region ($R_w < 0.5$), the normalized adhesion change ($R_a$) was greater than 1. The parameter sets in the low (repressed) Wnt signaling region that are the major population (93%) of $S_1$ could well explain experimental data. The minor population (7%) of $S_1$ that represents alternative models was rejected. This analysis shows that the model is robust over a wide range of parameters and that the model outputs are determined by the structure of the model rather than specific parameter values.

Although E-cadherin expression at membrane compartment is enhanced by Wnt stimulus in cells that contain normal APC, E-cadherin expression is transcriptionally repressed by Wnt signaling in APC mutated cells that contain only one allele of the mutated APC gene (Conacci-Sorrell et al., 2003; Smith et al., 1993). This means that Wnt stimulus should reduce E-cadherin expression when functional APC level is very low.

These qualitative experimental data provide additional constraints to select reference parameter set as follows:

$$R_w < 0.5 \text{ and } S_E < 0$$

where $R_w$ is the normalized Wnt response and $S_E$ is the sensitivity of E-cadherin expression to a small perturbation of β-catenin level when APC level is very low (i.e. APC level is 1% of its reference level), respectively. A negative sign of $S_E$ means that E-cadherin expression is decreased by additional β-catenin. Using these additional constraints, a reference parameter set was selected from the group ($S_1$), which is presented in Table S1.

To examine the robustness of the mathematical model with the estimated parameter set, we investigated local and global sensitivities (Figure S2B-D). Local sensitivity was defined as the relative change in the steady state level of output when a small perturbation (±1 %) was given to each parameter. The relative sensitivity coefficient for *i*-th kinetic parameter was calculated according to the following formula:

$$S_i = \frac{\partial y}{\partial p_i} \cdot \frac{p_i}{y}$$

where $y$ is the output of the mathematical model defined by the ratio of [adhesion complex] to [signaling complex] and $p_i$ is *i*-th kinetic parameter. From local sensitivity analysis, we found that the steady state of the system is sensitive to the parameters, $k_{8f/r}$ (APC-β-catenin binding), $k_{9f/r}$ (TCF-β-catenin binding), $k_{10}$ (APC shuttling), $k_{18}$ (internalization of ubiquitinated adhesion complex), although the system is robust to all other parameters (Figure S2B).

Local sensitivity analysis examines the sensitivity of the model with respect to single parameter changes. However, in real biological systems multiple parameter changes can occur simultaneously. So, we need to further investigate global sensitivity by varying multiple parameters randomly (Zi, 2011). An objective function for the global sensitivity analysis (GSA) is defined such that it returns 1 (acceptable) if additional β-catenin increases the adhesion level, or it returns -1 (unacceptable), if additional β-catenin decreases the adhesion level, because the main hypothesis depends on adhesion enhancement by additional β-catenin. For each parameter, the frequency of 'acceptable' or 'unacceptable' is presented with a blue or red line, respectively (Figure S2C,D). As a result, we found that the number of 'acceptables' was more than 80% for given parameters except $k_4$ and $K_{e50}$ (Figure S2C). In the subcellular model the major prediction was that Wnt stimulus enhances E-cadherin-mediated adhesion, as well as Wnt signaling. In case of protein abundance, the frequency of 'acceptables' decreases below 80% if the total amount of

TCF increases more than 3 fold of its reference value (Figure S2D).

**Step 3. Parameter selection using qualitative experimental data for the IMC model.**

To this date, only qualitative experimental data are available for the Wnt and APC profiles. Hence, we had to investigate if the IMC model can reproduce the β-catenin, E-cadherin, and Wnt activities along the crypt with the profiles of APC expression and Wnt ligands with random coefficients (Figure 3D-F). More than 85% of the random coefficients were concordant with the experimental molecular profiles of β-catenin, E-cadherin, and Wnt activity (Figures 3H,I and Figure S3B,C) (Fevr et al., 2007). This means that the model does not depend on its specific parameter value, and the model structure well explains experimental observations with respect to the profiles of β-catenin, E-cadherin, and Wnt activity along the crypt. The model predicted that all parameters that were concordant with the experimental profiles (β-catenin, E-cadherin, and Wnt activity) showed increased adhesion (adhesion complex) along the crypt (Figure 3G,J).

By using the genetic algorithm, we selected a reference coefficient set such that APC expression and Wnt ligand profiles fit the experimental profiles, where $W_{Max} = 55.98$, $\alpha_{Wnt} = 0.22$, $APC_{Min} = 5.22$, $A = 260.38$, $\alpha_{APC} = 0.44$, and $APC_{Max} = 238.77$, respectively.

# SUPPLEMENTAL REFERENCES


Aguilera, O., Fraga, M.F., Ballestar, E., Paz, M.F., Herranz, M., Espada, J., García, J.M., Muñoz, A., Esteller, M., and González-Sancho, J.M. (2006). Epigenetic inactivation of the Wnt antagonist DICKKOPF-1 (DKK-1) gene in human colorectal cancer. Oncogene *25*, 4116-4121.

Anderson, C.B., Neufeld, K.L., and White, R.L. (2002). Subcellular distribution of Wnt pathway proteins in normal and neoplastic colon. Proceedings of the National Academy of Sciences of the United States of America *99*, 8683-8688.

Aust, D.E., Terdiman, J.P., Willenbucher, R.F., Chew, K., Ferrell, L., Florendo, C., Molinaro-Clark, A., Baretton, G.B., Löhrs, U., and Waldman, F.M. (2001). Altered Distribution of β-Catenin, and Its Binding Proteins E-Cadherin and APC, in Ulcerative Colitis–Related Colorectal Cancers. Modern Pathology *14*, 29-39.

Batlle, E., Henderson, J.T., Beghtel, H., van den Born, M.M.W., Sancho, E., Huls, G., Meeldijk, J., Robertson, J., van de Wetering, M., Pawson, T., *et al.* (2002). Beta-catenin and TCF mediate cell positioning in the intestinal epithelium by controlling the expression of EphB/ephrinB. Cell *111*, 251-263.

Bienz, M. (1999). APC: the plot thickens. Current Opinion in Genetics & Development *9*, 595-603.

Bienz, M., and Clevers, H. (2003). Armadillo/β-catenin signals in the nucleus - Proof beyond a reasonable doubt? Nature Cell Biology *5*, 179-182.

Bienz, M., and Hamada, F. (2004). Adenomatous polyposis coli proteins and cell adhesion. Current Opinion in Cell Biology *16*, 528-535.

Bradley, R.S., Cowin, P., and Brown, A.M.C. (1993). Expression of Wnt-1 in PC12 cells results in modulation of plakoglobin and E-cadherin and increased cellular adhesion. Journal of Cell Biology *123*, 1857-1865.

Caldwell, G.M., Jones, C., Gensberg, K., Jan, S., Hardy, R.G., Byrd, P., Chughtai, S., Wallis, Y., Matthews, G.M., and Morton, D.G. (2004). The Wnt antagonist sFRP1 in colorectal tumorigenesis. Cancer Res *64*, 883-888.

Carothers, A.M., Melstrom, K.A., Jr., Mueller, J.D., Weyant, M.J., and Bertagnolli, M.M. (2001). Progressive changes in adherens junction structure during intestinal adenoma formation in Apc mutant mice. J Biol Chem *276*, 39094-39102.

Conacci-Sorrell, M., Simcha, I., Ben-Yedidia, T., Blechman, J., Savagner, P., and Ben-Ze'Ev, A. (2003). Autoregulation of E-cadherin expression by cadherin-cadherin interactions: The roles of β-catenin signaling, Slug, and MAPK. Journal of Cell Biology *163*, 847-857.

Corso, G., Marrelli, D., Pascale, V., Vindigni, C., and Roviello, F. (2012). Frequency of CDH1 germline mutations in gastric carcinoma coming from high- and low-risk areas: metanalysis and systematic review of the literature. BMC Cancer *12*.

De Beco, S., Gueudry, C., Amblard, F., and Coscoy, S. (2009). Endocytosis is required for E-cadherin redistribution at mature adherens junctions. Proceedings of the National Academy of Sciences of the United States of America *106*, 7010-7015.

Duguay, D., Foty, R.A., and Steinberg, M.S. (2003). Cadherin-mediated cell adhesion and tissue segregation: qualitative and quantitative determinants. Developmental Biology *253*, 309-323.

Escaffit, F., Perreault, N., Jean, D., Francoeur, C., Herring, E., Rancourt, C., Rivard, N., Vachon, P.H., Paré, F., Boucher, M.P., *et al.* (2005). Repressed E-cadherin expression in the lower crypt of human small intestine: A cell marker of functional relevance. Experimental Cell Research *302*, 206-220.

Faux, M.C., Ross, J.L., Meeker, C., Johns, T., Ji, H., Simpson, R.J., Layton, M.J., and Burgess, A.W. (2004). Restoration of full-length adenomatous polyposis coli (APC) protein in a colon cancer cell line enhances cell adhesion. Journal of Cell Science *117*, 427-439.

Fevr, T., Robine, S., Louvard, D., and Huelsken, J. (2007). Wnt/β-catenin is essential for intestinal homeostasis and maintenance of intestinal stem cells. Molecular and Cellular Biology *27*, 7551-7559.

Fodde, R., Smits, R., and Clevers, H. (2001). APC, signal transduction and genetic instability in colorectal cancer. Nature Reviews Cancer *1*, 55-67.

Foty, R.A., and Steinberg, M.S. (2005). The differential adhesion hypothesis: A direct evaluation. Developmental Biology *278*, 255-263.

Fujita, Y., Krause, G., Scheffner, M., Zechner, D., Leddy, H.E.M., Behrens, J., Sommer, T., and Birchmeier, W. (2002). Hakai, a c-Cbl-like protein, ubiquitinates and induces endocytosis of the

E-cadherin complex. Nat Cell Biol *4*, 222-231.

Gaspar, C., and Fodde, R. (2004). APC dosage effects in tumorigenesis and stem cell differenti ation. Int J Dev Biol *48*, 377-386.

González-Sancho, J.M., Aguilera, O., García, J.M., Pendás-Franco, N., Peña, C., Cal, S., Garcí a de Herreros, A., Bonilla, F., and Muñoz, A. (2005). The Wnt antagonist DICKKOPF-1 gene is a downstream target of beta-catenin/TCF and is downregulated in human colon cancer. Oncogen e *24*, 1098-1103.

Hülsken, J., Birchmeier, W., and Behrens, J. (1994). E-cadherin and APC compete for the inter action with β-catenin and the cytoskeleton. Journal of Cell Biology *127*, 2061-2069.

Hamada, F., and Bienz, M. (2002). A Drosophila APC tumour suppressor homologue functions in cellular adhesion. Nature Cell Biology *4*, 208-213.

Hammerschmidt, M., and Wedlich, D. (2008). Regulated Adhesion as a Driving Force of Gastr ulation Movements. Development *135*, 3625-3641.

Han, J.I., Kim, Y., Kim, D.Y., and Na, K.J. (2013). Alteration in E-Cadherin/β-Catenin Express ion in Canine Melanotic Tumors. Vet Pathol *50*, 274-280.

Hannoush, R.N. (2008). Kinetics of Wnt-driven β-catenin stabilization revealed by quantitativ e and temporal imaging. PLoS ONE *3*.

Hardt, S.v.d., Bakkers, J., Inbal, A., Carvalho, L., Solnica-Krezel, L., Heisenberg, C.-P., and H ammerschmidt, M. (2007). The Bmp Gradient of the Zebrafish Gastrula Guides Migrating Latera l Cells by Regulating Cell-Cell Adhesion. Current Biology *17*, 475-487.

Harris, T.J.C., and Tepass, U. (2010). Adherens junctions: from molecules to morphogenesis. Nat Rev Mol Cell Biol *11*, 502-514.

Heath, J.P. (1996). Epithelial cell migration in the intestine. Cell Biol Int *20*, 139-146.

Hendriksen, J., Jansen, M., Brown, C.M., van der Velde, H., van Ham, M., Galjart, N., Offerha us, G.J., Fagotto, F., and Fornerod, M. (2008). Plasma membrane recruitment of dephosphorylate d β-catenin upon activation of the Wnt pathway. Journal of Cell Science *121*, 1793-1802.

Herzig, M., Savarese, F., Novatchkova, M., Semb, H., and Christofori, G. (2007). Tumor progr ession induced by the loss of E-cadherin independent of β-catenin/Tcf-mediated Wnt signaling. Oncogene *26*, 2290-2298.

Hinck, L., Nelson, W.J., and Papkoff, J. (1994). Wnt-1 modulates cell-cell adhesion in mamma lian cells by stabilizing β- catenin binding to the cell adhesion protein cadherin. Journal of Cell B iology *124*, 729-741.

Hirokawa, N., and Noda, Y. (2008). Intracellular transport and kinesin superfamily proteins, K IFs: Structure, function, and dynamics. Physiological Reviews *88*, 1089-1118.

Huber, A.H., Stewart, D.B., Laurents, D.V., Nelson, W.J., and Weis, W.I. (2001). The cadherin cytoplasmic domain is unstructured in the absence of β-catenin. A possible mechanism for regula ting cadherin turnover. Journal of Biological Chemistry *276*, 12301-12309.

Humphries, A., and Wright, N.A. (2008). Colonic crypt organization and tumorigenesis. Natur e Reviews Cancer *8*, 415-424.

Ishiyama, N., Lee, S.H., Liu, S., Li, G.Y., Smith, M.J., Reichardt, L.F., and Ikura, M. (2010). D ynamic and Static Interactions between p120 Catenin and E-Cadherin Regulate the Stability of C ell-Cell Adhesion. Cell *141*, 117-128.

Iwamoto, M., Ahnen, D.J., Franklin, W.A., and Maltzman, T.H. (2000). Expression of β-cateni n and full-length APC protein in normal and neoplastic colonic tissues. Carcinogenesis *21*, 1935-1940.

Iwao, K., Nakamori, S., Kameyama, M., Imaoka, S., Kinoshita, M., Fukui, T., Ishiguro, S., Na

kamura, Y., and Miyoshi, Y. (1998). Activation of the β-Catenin Gene by Interstitial Deletions In volving Exon 3 in Primary Colorectal Carcinomas without Adenomatous Polyposis Coli Mutatio ns. Cancer Res *58*, 1021-1026.

Jamora, C., DasGupta, R., Kocieniewski, P., and Fuchs, E. (2003). Links between signal transd uction, transcription and adhesion in epithelial bud development. Nature *422*, 317-322.

Jeanes, A., Gottardi, C.J., and Yap, A.S. (2008). Cadherins and cancer: How does cadherin dys function promote tumor progression? Oncogene *27*, 6920-6929.

Jimbo, T., Kawasaki, Y., Koyama, R., Sato, R., Takada, S., Haraguchi, K., and Akiyama, T. (20 02). Identification of a link between the tumour suppressor APC and the kinesin superfamily. Nat Cell Biol *4*, 323-327.

Kawanishi, J., Kato, J., Sasaki, K., Fujii, S., Watanabe, N., and Niitsu, Y. (1995). Loss of E-ca dherin-dependent cell-cell adhesion due to mutation of the beta-catenin gene in a human cancer c ell line, HSC-39. Molecular and Cellular Biology *15*, 1175-1181.

Kicheva, A., Pantazis, P., Bollenbach, T., Kalaidzidis, Y., Bittig, T., Jülicher, F., and González-Gaitán, M. (2007). Kinetics of morphogen gradient formation. Science *315*, 521-525.

Klingelhöfer, J., Troyanovsky, R.B., Laur, O.Y., and Troyanovsky, S. (2003). Exchange of cate nins in cadherin-catenin complex. Oncogene *22*, 1181-1188.

Kuphal, F., and Behrens, J. (2006). E-cadherin modulates Wnt-dependent transcription in color ectal cancer cells but does not alter Wnt-independent gene expression in fibroblasts. Experimenta l Cell Research *312*, 457-467.

Le, T.L., Yap, A.S., and Stow, J.L. (1999). Recycling of E-cadherin: a potential mechanism for regulating cadherin dynamics. J Cell Biol *146*, 219-232.

Lecuit, T., and Lenne, P.F. (2007). Cell surface mechanics and the control of cell shape, tissue patterns and morphogenesis. Nature Reviews Molecular Cell Biology *8*, 633-644.

Lee, E., Salic, A., Krüger, R., Heinrich, R., and Kirschner, M.W. (2003). The roles of APC and axin derived from experimental and theoretical analysis of the Wnt pathway. PLoS Biology *1*.

Leedham, S.J., Rodenas-Cuadrado, P., Howarth, K., Lewis, A., Mallappa, S., Segditsas, S., Da vis, H., Jeffery, R., Rodriguez-Justo, M., Keshav, S*., et al.* (2012). A basal gradient of Wnt and st em-cell number influences regional tumour distribution in human and mouse intestinal tracts. Gu t.

Long, Q., Zhang, X., and Bostick, R.M. (2011). Semiparametric Estimation for Joint Modeling of Colorectal Cancer Risk and Functional Biomarkers Measured with Errors. Biom J *53*, 393-41 0.

Ma, L., Young, J., Prabhala, H., Pan, E., Mestdagh, P., Muth, D., Teruya-Feldstein, J., Reinhar dt, F., Onder, T.T., Valastyan, S*., et al.* (2010). miR-9, a MYC/MYCN-activated microRNA, regu lates E-cadherin and cancer metastasis. Nature cell biology *12*, 247-256.

MacDonald, B.T., Tamai, K., and He, X. (2009). Wnt/β-Catenin Signaling: Components, Mech anisms, and Diseases. Developmental Cell *17*, 9-26.

Medema, J.P., and Vermeulen, L. (2011). Microenvironmental regulation of stem cells in intest inal homeostasis and cancer. Nature *474*, 318-326.

Midgley, C.A., White, S., Howitt, R., Save, V., Dunlop, M.G., Hall, P.A., Lane, D.P., Wyllie, A. H., and Bubb, V.J. (1997). APC expression in normal human tissues. J Pathol *181*, 426-433.

Mimori-Kiyosue, Y., Shiina, N., and Tsukita, S. (2000). Adenomatous polyposis coli (APC) pr otein moves along microtubules and concentrates at their growing ends in epithelial cells. Journal of Cell Biology *148*, 505-517.

Moran, U., Phillips, R., and Milo, R. (2010). SnapShot: key numbers in biology. Cell *141*, 126

2-1262.e1261.

Morin, P.J., Sparks, A.B., Korinek, V., Barker, N., Clevers, H., Vogelstein, B., and Kinzler, K. W. (1997). Activation of β-Catenin-Tcf Signaling in Colon Cancer by Mutations in β-Catenin or APC. Science *275*, 1787-1790.

Nagafuchi, A., Shirayoshi, Y., Okazaki, K., Yasuda, K., and Takeichi, M. (1987). Transformati on of cell adhesion properties by exogenously introduced E-cadherin cDNA. , Published online: 24 September 1987; | doi:101038/329341a0 *329*, 341-343.

Nagafuchi, A., and Takeichi, M. (1988). Cell binding function of E-cadherin is regulated by th e cytoplasmic domain. EMBO J *7*, 3679-3684.

Najdi, R., Holcombe, R.F., and Waterman, M.L. (2011). Wnt signaling and colon carcinogenes is: beyond APC. J Carcinog *10*, 5.

Nelson, W.J., and Nusse, R. (2004). Convergence of Wnt, β-Catenin, and Cadherin pathways. Science *303*, 1483-1487.

Neufeld, K.L., Zhang, F., Cullen, B.R., and White, R.L. (2000). APC-mediated downregulatio n of β-catenin activity involves nuclear sequestration and nuclear export. EMBO Reports *1*, 519-523.

Orsulic, S., Huber, O., Aberle, H., Arnold, S., and Kemler, R. (1999). E-cadherin binding prev ents β-catenin nuclear localization and β-catenin/LEF-1-mediated transactivation. Journal of Cell Science *112*, 1237-1245.

Papkoff, J., Rubinfeld, B., Schryver, B., and Polakis, P. (1996). Wnt-1 regulates free pools of c atenins and stabilizes APC-catenin complexes. Molecular and Cellular Biology *16*, 2128-2134.

Park, J.K., Song, J.H., He, T.C., Nam, S.W., Lee, J.Y., and Park, W.S. (2009). Overexpression of Wnt-2 in colorectal cancers. Neoplasma *56*, 119-123.

Pece, S., and Gutkind, J.S. (2002). E-cadherin and Hakai: signalling, remodeling or destructio n? Nat Cell Biol *4*, E72-E74-E72-E74.

Phelps, R.A., Chidester, S., Dehghanizadeh, S., Phelps, J., Sandoval, I.T., Rai, K., Broadbent, T., Sarkar, S., Burt, R.W., and Jones, D.A. (2009). A two-step model for colon adenoma initiation and progression caused by APC loss. Cell *137*, 623-634.

Rubinfeld, B., Souza, B., Albert, I., Munemitsu, S., and Polakis, P. (1995). The APC protein an d E-cadherin form similar but independent complexes with α-catenin, β-catenin, and plakoglobin. Journal of Biological Chemistry *270*, 5549-5555.

Sansom, O.J., Meniel, V.S., Muncan, V., Phesse, T.J., Wilkins, J.A., Reed, K.R., Vass, J.K., At hineos, D., Clevers, H., and Clarke, A.R. (2007). Myc deletion rescues Apc deficiency in the sma ll intestine. Nature *446*, 676-679.

Senda, T., Iizuka-Kogo, A., Onouchi, T., and Shimomura, A. (2007). Adenomatous polyposis c oli (APC) plays multiple roles in the intestinal and colorectal epithelia. Med Mol Morphol *40*, 6 8-81.

Smith, K., Bui, T.D., Poulsom, R., Kaklamanis, L., Williams, G., and Harris, A.L. (1999). Up-r egulation of macrophage wnt gene expression in adenoma-carcinoma progression of human colo rectal cancer. Br J Cancer *81*, 496-502.

Smith, K.J., Johnson, K.A., Bryan, T.M., Hill, D.E., Markowitz, S., Willson, J.K., Paraskeva, C., Petersen, G.M., Hamilton, S.R., and Vogelstein, B. (1993). The APC gene product in normal a nd tumor cells. PNAS *90*, 2846-2850.

Steinberg, M.S. (2007). Differential adhesion in morphogenesis: a modern view. Current Opini on in Genetics and Development *17*, 281-286.

Stepniak, E., Radice, G.L., and Vasioukhin, V. (2009). Adhesive and Signaling Functions of Ca

dherins and Catenins in Vertebrate Development. Cold Spring Harbor Perspectives in Biology *1*.

Suzuki, H., Watkins, D.N., Jair, K.W., Schuebel, K.E., Markowitz, S.D., Chen, W.D., Pretlow, T.P., Yang, B., Akiyama, Y., Van Engeland, M.*, et al.* (2004). Epigenetic inactivation of SFRP ge nes allows constitutive WNT signaling in colorectal cancer. Nat Genet *36*, 417-422.

Tan, C.W., Gardiner, B.S., Hirokawa, Y., Layton, M.J., Smith, D.W., and Burgess, A.W. (2012). Wnt Signalling Pathway Parameters for Mammalian Cells. PLoS ONE *7*.

Toyofuku, T., Hong, Z., Kuzuya, T., Tada, M., and Hori, M. (2000). Wnt/frizzled-2 signaling i nduces aggregation and adhesion among cardiac myocytes by increased cadherin-β-catenin comp lex. Journal of Cell Biology *150*, 225-241.

van de Wetering, M., Sancho, E., Verweij, C., de Lau, W., Oving, I., Hurlstone, A., van der Ho rn, K., Batlle, E., Coudreuse, D., Haramis, A.P.*, et al.* (2002). The beta-catenin/TCF-4 complex i mposes a crypt progenitor phenotype on colorectal cancer cells. Cell *111*, 241-250.

van Leeuwen, I.M.M., Byrne, H.M., Jensen, O.E., and King, J.R. (2007). Elucidating the inter actions between the adhesive and transcriptional functions of β-catenin in normal and cancerous cells. Journal of Theoretical Biology *247*, 77-102.

von Kries, J.P., Winbeck, G., Asbrand, C., Schwarz-Romond, T., Sochnikova, N., Dell'Oro, A., Behrens, J., and Birchmeier, W. (2000). Hot spots in β-catenin for interactions with LEF-1, cond uctin and APC. Nat Struct Mol Biol *7*, 800-807.

Wijnhoven, B.P., Dinjens, W.N., and Pignatelli, M. (2000). E-cadherin-catenin cell-cell adhesi on complex and human cancer. The British Journal of Surgery *87*, 992-1005.

Wu, X., Tu, X., Joeng, K.S., Hilton, M.J., Williams, D.A., and Long, F. (2008). Rac1 activatio n controls nuclear localization of beta-catenin during canonical Wnt signaling. Cell *133*, 340-353.

Yokoyama, N., Yin, D., and Malbon, C.C. (2007). Abundance, complexation, and trafficking o f Wnt/β-catenin signaling elements in response to Wnt3a. Journal of Molecular Signaling *2*.

Zhu, M., Tang, D., Wu, Q., Hao, S., Chen, M., Xie, C., Rosier, R.N., O'Keefe, R.J., Zuscik, M., and Chen, D. (2009). Activation of β-Catenin Signaling in Articular Chondrocytes Leads to Oste oarthritis-Like Phenotype in Adult β-Catenin Conditional Activation Mice. J Bone Miner Res *24*, 12-21.

Zi, Z. (2011). Sensitivity analysis approaches applied to systems biology models. IET Systems Biology *5*, 336-346.